

SilentWood: Efficient Private Inference Over Gradient Boosting Decision Forests

Ronny Ko
LG Electronics
Seoul, South Korea
hajoon.ko@lge.com

Abdelkarim Kati
University of Waterloo
Canada
akati@uwaterloo.ca

Robin Geelen
KU Leuven
belgium
robin.geelen@esat.kuleuven.be

Rasoul Akhavan Mahdavi
University of Waterloo
Canada
r5akhava@uwaterloo.ca

Byoungwoo Yoon
LG Electronics
South Korea
byoungwoo.yoon@lge.com

Jongho Shin
LG Electronics
South Korea
jongho0.shin@lge.com

Anton Jappinen
LG Electronics
South Korea
anton.yappinen@lge.com

Igor Moroz
LG Electronics
South Korea
igormoroz1969@gmail.com

Zhiqiang Lin
Ohio State University
USA
zlin@cse.ohio-state.edu

Makoto Onizuka
Osaka University
Japan
onizuka@ist.osaka-u.ac.jp

Florian Kerschbaum
University of Waterloo
Canada
fkerschb@uwaterloo.ca

Abstract

Gradient boosting decision forests, used by XGBoost or AdaBoost, offer higher accuracy and lower training times than decision trees for large datasets. Protocols for private inference over decision trees can be used to preserve the privacy of the input data as well as the privacy of the trees. However, naively extending private inference over decision trees to private inference over decision forests by replicating the protocols leads to impractical running times. In this paper, we propose an efficient private decision inference protocol using homomorphic encryption. We present several optimizations that identify and then remove (approximate) duplication between the trees in a forest, thereby achieving significant improvements in communication and computation cost over the naive approach. To the best of our knowledge, we present the first private inference protocol for highly scalable gradient boosting decision forests. Our protocol's (SilentWood) inference time is faster than the baseline of parallel running the RCC-PDTE protocol by Mahdavi et al. by up to 42.5x, and faster than Zama's Concrete ML [53] XGBoost by up to 27.8x, and faster than SoK-GGG's two-party garbled circuit protocol by 2.94x.

Permission to make digital or hard copies of all or part of this work for personal or classroom use is granted without fee provided that copies are not made or distributed for profit or commercial advantage and that copies bear this notice and the full citation on the first page. Copyrights for components of this work owned by others than the author(s) must be honored. Abstracting with credit is permitted. To copy otherwise, or republish, to post on servers or to redistribute to lists, requires prior specific permission and/or a fee. Request permissions from permissions@acm.org.

Conference'25, Washington, Taipei, Taiwan

© 2026 Copyright held by the owner/author(s). Publication rights licensed to ACM.

ACM ISBN 978-x-xxxx-xxxx-x/YYYY/MM

<https://doi.org/10.1145/nnnnnnn.nnnnnnn>

1 Introduction

Machine Learning as a Service (MLaaS) allows large user groups to use machine learning models. A service provider trains a model and offers users inference using this model. Some of such examples include recommendation systems, spam filtering, and object detection used in e-commerce services, social networking services, and smart home. An advantage of such MLaaS is that the provider can control access to the model and easily update it when new training data is available. In contrast, its disadvantage is the privacy concern of the users revealing their test data to the provider which may be sensitive or legally restricted. Cryptography offers a compelling solution to this problem. The user can encrypt its data, e.g., using fully homomorphic encryption [25, 31], and the provider can perform private inference. However, this solution usually has high computational costs. Alternatively, the user and the provider can engage in a two-party computation [43, 51, 52] where the user's input is computed through the model in a *blinded* manner, during which the server's trained model parameters and the user's private data are not leaked to each other. However, a drawback of two-party computation is that it usually incurs high communication costs.

In this paper, we develop a new protocol for private inference over gradient boosting decision forests, which are collections of decision trees whose results are combined into the final model prediction. Gradient boosting forests offer a better trade-off between higher accuracy and lower training time than training a single decision tree for large datasets. Moreover, they retain a critical advantage of decision trees over many other machine learning techniques; their predictions are explainable, helping to fulfill legal, social, and ethical requirements.

Many private inference protocols over decision trees exist, e.g., [3–6, 9, 12, 16, 19, 29, 33–35, 39, 45–47, 49] (§6). However, extending

these to gradient boosting decision forests comes with two challenges. First, the results of the decision trees need to be combined into a single prediction result, requiring further computation. This can particularly pose a problem for protocols using homomorphic encryption [3, 9, 19, 34, 46, 49], since these computations increase the multiplication overhead, significantly increasing the runtime of the protocols. Second, even naively running several independent decision tree protocols without combining their results can exhaust the server's computing resources. Therefore, optimizations are necessary to reduce the cost of executing multiple decision tree evaluations on the same input.

To solve these problems, we propose SilentWood, a private inference protocol for gradient boosting that uses three novel techniques. First, to reduce the high computation overhead caused by frequent homomorphic rotations in FHE-based PDTE (private decision tree evaluation), SilentWood applies node clustering (i.e., grouping and weighted-averaging tree nodes having similar thresholds) and path clustering (i.e., combining tree paths having the same path conditions) to eliminate redundant computations (§4.1). Second, SilentWood proposes the Blind Code Conversion (BCC) protocol to address the incompatibility of SumPath (and the high cost issue of Multiply-Path) for score aggregation of gradient boosting models (§4.2). BCC is a lightweight two-party protocol in which the server pads and shuffles its intermediate ciphertext to make the plaintext contents appear uniformly random from the user's perspective. The user's role is to decrypt it and convert the underlying plaintext values *blindly* to help the server's subsequent computation of score aggregation. This process ensures the information in the intermediate ciphertext to be inaccessible from both the client and server, while realizing arithmetic compatibility of the server's score aggregation. Lastly, to reduce communication overhead caused by repetitive data encoding in FHE-based PDTE, SilentWood's ciphertext compression carefully removes repetitive encodings before encryption and then homomorphically restores the original data format on the server side (i.e., homomorphic decompression), thus minimizing ciphertext size while preserving necessary SIMD comparisons (§4.3).

Although most of our contributions are independent of the specific PDTE protocols used and are also applicable to many other protocols that use homomorphic encryption, we extend RCC-PDTE [3] (§A), a state-of-the-art PDTE protocol that uses FHE. While RCC-PDTE is effective for computing a single decision tree, naively repeating this protocol for all decision trees (100 in our default setup) can take more than 5 minutes for a single inference, which is prohibitively long. The inference time of SilentWood is faster than this baseline by up to 42.5x, faster than Zama's Concrete ML [53] XGBoost by up to 34.0x, and faster than SoK-GGG (i.e., a state-of-the-art MPC protocol based on GC) by 2.94x (§5).

Our paper's contributions are as follows:

- We propose three optimization techniques for efficient private inference of random forest models: computation clustering, blind code conversion, and ciphertext compression.
- We implemented SilentWood, a prototype of our proposed techniques.
- We provide evaluation results of SilentWood and compare it to other state-of-the-art protocols.

2 Background

2.1 Gradient Boosting Models

Ensemble decision trees [7] is a machine learning technique that combines multiple small trees as weak learners to improve overall prediction. There are two types of ensemble methods: random forests [11] and gradient boosting [28]. Random forests build multiple trees independently and make the final prediction by aggregating the predictions from individual trees (e.g., voting or averaging). Gradient boosting also builds multiple trees, but sequentially, to incrementally correct the errors of the previous ones and collectively build a strong model through incremental improvement. XGBoost [15] and AdaBoost [27] are among the most widely used gradient boosting algorithms. In this work, we focus on private inference of these two boosted decision tree models.

In AdaBoost, each trained tree is assigned a weight, and each leaf node is assigned a sign, where '+' and '-' correspond to binary classes. The inference procedure is as follows: (1) traverse each tree from the root node by comparing the client's feature input values with the threshold values at each node; (2) reach and retrieve the leaf node's value; (3) multiply it by the weight assigned to its tree; (4) sum all such intermediate values computed from all trees; and (5) determine the sign (+/-) of the final summed value as the inferred binary class.

XGBoost supports both binary and multi-class classification. For binary classification, it sums the leaf node values of all traversed trees, applies the sigmoid function to this sum, and then determines the binary class based on whether the computed sigmoid value is greater than 0.5. For multi-class classification, it sums the leaf node values of all traversed trees corresponding to each class, obtaining a summed value for each class. We then apply the softmax function to these summed results and determine the class with the maximum softmax value as the inferred class.

2.2 Fully Homomorphic Encryption (FHE)

Fully Homomorphic Encryption (FHE)[30] is a cryptographic scheme that allows addition or multiplication of encrypted plaintexts without decrypting them. Among various FHE schemes, SilentWood uses an RLWE-family scheme (specifically BFV[26]) due to its efficient support for SIMD (Single Instruction Multiple Data) operations. In this scheme, the granularity of operation is a vector of elements, where each element is a plaintext value. To use the RLWE-family scheme, we first encode (Encode) the n -dimensional plaintext input vector into an $(n - 1)$ -degree polynomial $M(X)$, and then encrypt (Encrypt) the polynomial into an RLWE ciphertext using a secret key polynomial $S(X)$ as $\text{RLWE}_{S(X)}(M(X))$. Given such ciphertexts, we can perform cipher-plaintext addition (PAdd) between an RLWE ciphertext and a plaintext polynomial, cipher-cipher addition between two RLWE ciphertexts, cipher-plaintext multiplication, cipher-cipher multiplication, and rotation (in a round-robin manner) of the plaintext vector elements encrypted in a ciphertext, all without decrypting them. The standard FHE operations are summarized as follows:

- (1) $\text{Encode}([v_0, v_1, \dots, v_{n-1}]) \triangleright$ each $v_i \in \mathbb{Z}_t$ for plaintext modulus t
 $\rightarrow M(X) \triangleright M(X) \in \mathbb{Z}_t[X]/(X^n + 1)$
- (2) $\text{Decode}(M(X)) \rightarrow [v_0, v_1, \dots, v_{n-1}]$

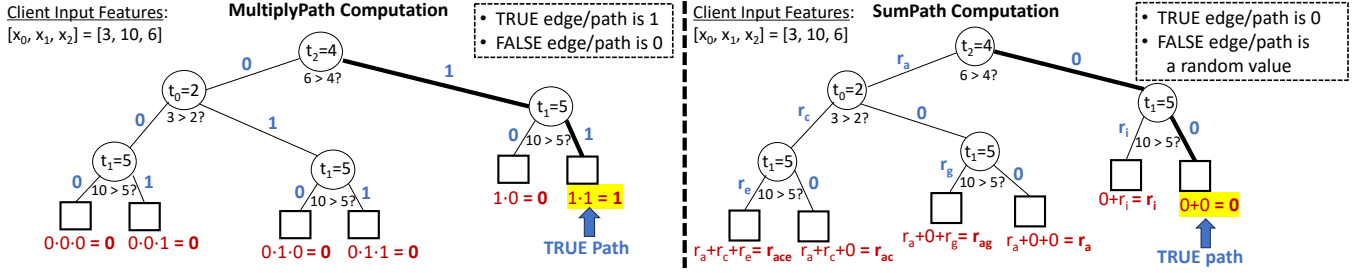


Figure 1: Computation of MultiplyPath and SumPath

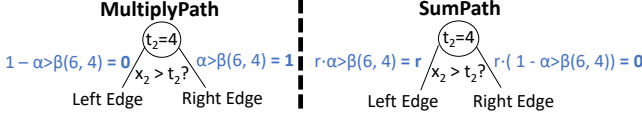


Figure 2: Edge formulas for SumPath and MultiplyPath

- (3) $\text{Encrypt}(M(X), pk) \rightarrow ct \triangleright$ a ciphertext that encrypts $\Delta \cdot M(X)$ under $sk = S(X) \in \{-1, 0, 1\}^n \subset \mathbb{Z}[X]/(X^n + 1)$
- (4) $\text{Decrypt}(ct, sk) \rightarrow M(X)$
- (5) $\text{PAdd}(ct_1, M_2(X)) \rightarrow ct \triangleright$ encrypts $\Delta \cdot (M_1(X) + M_2(X))$, which decodes to $\text{Decode}(M_1(X)) + \text{Decode}(M_2(X))$
- (6) $\text{CAdd}(ct_1, ct_2) \rightarrow ct \triangleright$ encrypts $\Delta \cdot (M_1(X) + M_2(X))$, which decodes to $\text{Decode}(M_1(X)) + \text{Decode}(M_2(X))$
- (7) $\text{PMult}(ct_1, M_2(X)) \rightarrow ct \triangleright$ encrypts $\Delta \cdot (M_1(X) \cdot M_2(X))$, which decodes to $\text{Decode}(M_1(X)) \odot \text{Decode}(M_2(X))$ (where \odot is element-wise vector multiplication)
- (8) $\text{CMult}(ct_1, ct_2) \rightarrow ct \triangleright$ encrypts $\Delta \cdot (M_1(X) \cdot M_2(X))$, which decodes to $\text{Decode}(M_1(X)) \odot \text{Decode}(M_2(X))$ (assuming CMult includes modulus switching to rescale $\Delta^2 \rightarrow \Delta$)
- (9) $\text{Rotate}(ct, r) \rightarrow ct' \triangleright$ if $\text{Decode}(M(X)) = [v_0, \dots, v_{n-1}]$, then $\text{Decode}(M'(X)) = [v_r, \dots, v_{n-1}, v_0, \dots, v_{r-1}]$

One important benefit of RLWE-family schemes is that their homomorphic addition and multiplication support efficient SIMD operations over the underlying plaintext vector. Upon addition or multiplication of two RLWE ciphertexts, the underlying vectors in the ciphertexts are added or multiplied element-wise, all at once. The same is true for cipher-plaintext computation: the encrypted vector in the RLWE ciphertext and the encoded vector in the RLWE plaintext are added or multiplied element-wise. In RLWE-family schemes, the typical dimension sizes of plaintext vectors are 2^{13} , 2^{14} , or 2^{15} , which essentially represent the level of parallelism in SIMD.

In this paper, we use the nine aforementioned FHE operations as black boxes to homomorphically compute the inference results of gradient boosting models.

2.3 Private Decision Tree Evaluation

Private Decision Tree Evaluation (PDTE) is a protocol between a server and a client. The client's input is a vector of values representing a sample data point, and the server's input is a decision forest. At the end of the protocol, the server learns nothing about the client's inputs, while the client learns nothing about the server's model other than the prediction result and the model's hyper-parameters (e.g.,

types of features and classes)¹. Among the returned class probabilities (i.e., scores), the client usually picks the class with the highest probability as the prediction, although it can apply more sophisticated algorithms in the case of near ties.

In this section, we overview existing PDTE techniques based on FHE. PDTE generally comprises two steps: value comparison between a feature and a threshold at each tree node (§ 2.3.1); and tree path evaluation (§ 2.3.2).

2.3.1 Value Comparison at Each Node. Traversing a decision tree at inference time requires *greater-than* comparisons between an input feature and a threshold at each tree node. However, as explained in §2.2, the only arithmetic operations directly supported by FHE are addition and multiplication (+, ·). Therefore, to homomorphically compare two numbers, one needs to design an arithmetic logic circuit comprising only (+, ·) operations such that the gate returns 1 if $\alpha > \beta$, and returns false if $\alpha \leq \beta$.

Given the input feature X node and threshold Y are n -bits long, one way to build a value comparison circuit is to encrypt each binary bit of X and Y as (x_1, x_2, \dots, x_n) and (y_1, y_2, \dots, y_n) and design the value comparator logic as follows:

- $\text{EQBit}(a, b) = 1 - a - b \pmod{2} \triangleright$ bit a is equal to bit b
- $\text{GTBit}(a, b) = a \cdot (1 - b) \pmod{2} \triangleright$ bit $a > b$
- $\text{EQ}_{i \rightarrow j}(X, Y) = \prod_{j=i}^k \text{EQBit}(x_j, y_j)$
 \triangleright Are X, Y 's bits $i \sim k$ equal?
- $\text{GT}(X, Y) = \sum_{i=0}^{n-1} (\text{EQ}_{i+1 \rightarrow n-1}(X, Y) \cdot \text{GTBit}(x_i, y_i))$
 $\triangleright X > Y?$

Given the above setup, $\text{GT}(X, Y)$ returns 1 if $X > Y$; 0 otherwise. Since the above formulas comprise only addition and multiplication operations, they can be executed by using FHE. However, using a bit-wise comparator requires the later tree path evaluation operation (§ 2.3.2) to be performed also as a verbose binary circuit, which is not an optimal design for FHE. This is because binary circuits usually involve a deep multiplication chain and FHE requires an increasingly more computation time for a greater multiplication depth.

The state-of-the-art PDTE protocols design the comparison operator in a more efficient manner, such as based on constant-weight encoding [3]. This comparator's computation is done in reduction modulo p (which supports larger than even 20 bits), and also its size of multiplication depth is smaller. SilentWood leverages a comparison operator based on constant-weight (CW) encoding, which returns

¹More precisely, in PDTE, the server-side privacy goal is to leak the server's model information no more than its original plaintext inference protocol.

1 if the feature is greater than or equal to the threshold; returns 0 otherwise. The details of the algorithm are described in §A.

2.3.2 Tree Path Evaluation. After we have homomorphically compared the thresholds and input features at each tree node, we use each node’s (encrypted) comparison result to compute the path results. There are generally two ways to achieve this: MultiplyPath (i.e., path conjugation) [35] and SumPath [47]. Figure 2 depicts the left/right edge formulas for MultiplyPath and SumPath, respectively. The property of MultiplyPath edge formulas is that condition-satisfying true edges receive a value of 1, while false edges receive a value of 0, whereas in the case of the SumPath edge formulas, true edges receive a value of 0, and false edges receive a non-zero random number (r). Based on these edge formulas, Figure 1 shows how to compute the final path values. In the case of MultiplyPath, we compute each path’s final value by multiplying all the edge values that comprise the path. Therefore, the true path receives the final value of 1, whereas all other false paths receive the final value of 0. On the other hand, in the case of SumPath, we compute each path’s final value by summing all edge values that comprise the path. Therefore, the true path receives the final value of 0, whereas all other false paths receive a final value of some non-zero random number. SumPath can be evaluated more efficiently by FHE (as well as MPC) because it involves only addition operations, whereas MultiplyPath requires heavy multiplications, the frequency of which is as high as the length of each path.

Once all SumPath (or MultiplyPath) values are homomorphically computed for all paths, the server returns them to the client, who decrypts them and considers the leaf value having a SumPath of 0 as the final classification result.

3 Motivation

Applying existing PDTE methods results in a large computational overhead because handling many trees in decision forests is expensive. In this section, we illustrate three motivating challenges for efficient private decision forest evaluation.

[C1]: Many Tree Nodes and Paths. When we homomorphically compare a threshold and an input feature at each tree node, we run the $\alpha > \beta(X, Y)$ function (in Figure 9) in a SIMD manner using a large number of ciphertext slots; thus, multiple comparison results are stored across multiple slots in the ciphertext. After that, in order to prepare for computing SumPaths (or MultiplyPaths) based on these results, we need to clone as many ciphertexts as the number of unique [feature type, threshold value] pairs existing across all trees, each of which represents the associated node’s comparison result, and rotate the ciphertext to align all comparison results to the first slot in the plaintext vector for subsequent computations. We do this because FHE addition/multiplication operations are performed element-wise at the same slot index. Due to this requirement for comparison value alignment, existing PDTE techniques must perform as many homomorphic rotations as the number of unique [feature type, threshold value] pairs in all trees. Such a problem of having to run many rotations becomes critical in decision forests because there are not a single tree but many trees (e.g., 100 or even 1000) to compute, involving a large number of tree nodes and paths.

[C2]: Final Score Aggregation. In gradient boosting models, computing the final score requires summing the leaf values of all true

paths in many decision trees. A practical private evaluation method should meet two key requirements: (1) arithmetic compatibility with homomorphic evaluation; and (2) computational efficiency. Existing approaches fail to meet the two requirements simultaneously. In the case of SumPath [3], given a leaf node’s value, its associated SumPath value (either 0 or r), and $(+, \cdot)$ operations, there is no arithmetic formula to express the logic: $\text{SumPath} == 0 ? \text{leafValue} : 0$. In the case of MultiplyPath [19] whose values are either 1 or 0, the logic $\text{MultiplyPath} == 1 ? \text{leafValue} : 0$ can be expressed as the arithmetic formula $\text{MultiplyPath} \cdot \text{LeafValue}$. However, computing this formula requires as many homomorphic multiplications as the length of each path, which is computationally expensive.

[C3]: Huge Communication Cost. As the number of tree nodes increases, the required size of ciphertexts also increases due to bit-wise encoding and encryption. In the example of RCC-PDTE [3], a query ciphertext size of 85.7 MB is required for 32-bit precision of input features, in which case the majority of the inference runtime occurs in the network data transmission.

4 Our Protocol: SilentWood

In this section, we explain how SilentWood solves the challenges of efficiently evaluating private decision forests, especially gradient boosting models (i.e., XGBoost and AdaBoost). SilentWood’s innovation lies in efficiently computing the inference results of private gradient boosting models based on three novel techniques: computation clustering, ciphertext compression, and blind code conversion. SilentWood internally leverages RCC-PDTE’s value comparison (§A) and SumPath computation (§ 2.3.2) to evaluate decision trees.

Threat Model: Our privacy guaranty assumes a setup comprising a semi-honest client (i.e., follows the protocol) and a malicious server (i.e., may deviate from the protocol).² They try to learn about each other’s secrets from exchanged messages. The server’s secret is its trained gradient boosting model; the client’s secret is its input feature values. As common information, They know the feature names and feature bit-lengths. At the end of the communication, the server learns nothing about the client’s features; the client learns only the inference scores/probabilities for each class and the fact that the number of tree paths is bounded by a large constant defined in the hyperparameters. The client learns nothing about the server’s model (tree count, shape, depth, or node thresholds) except that the number of tree paths is capped at some multiple of the cyclotomic polynomial degree (e.g., 2^{14}).

4.1 Computation Clustering

As discussed in C1 in §3, one major challenge in private decision forest evaluation is reducing the computational overhead caused by a large number of homomorphic operations for threshold comparison and path evaluation. SilentWood reduces this overhead by introducing node & path clustering techniques, which combine the same or similar computations during inference across different trees to reduce the total number of computations.

4.1.1 Node Clustering. To reduce the overhead of homomorphic rotations, SilentWood’s first insight is to compute comparison results

²For the discussion of the alternative setup that assumes a malicious client and a malicious server, see §B

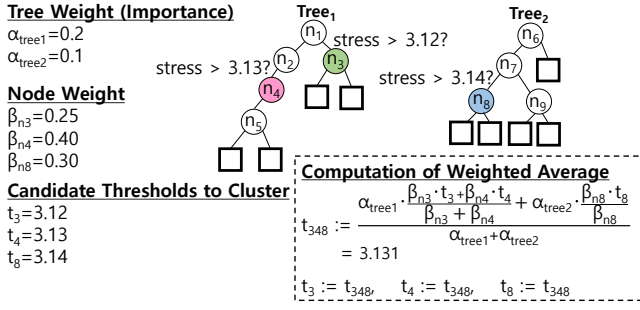


Figure 3: An examples of node clustering

only once for each distinct type of tree node (uniquely identified as [feature, threshold]) across all trees in the model, thereby eliminating redundant comparison operations. Afterward, these results can be used as building blocks to create the desired combinations of edges for each tree path in the model to compute all SumPath (or MultiplyPath) values. However, the benefit of this approach is limited because it can save comparison operations and rotations only for those nodes that have exactly the same threshold values.

To more actively eliminate the number of computations, SilentWood clusters those nodes that have not only the same threshold values but also similar threshold values and replaces them with their *weighted average*, where the contribution of each threshold is weighted by the weight of the tree and the node to which it belongs (will be detailed later). In Figure 3’s example, we have three tree nodes n_3 , n_4 , and n_8 , all having the same feature name (e.g., stress level) and similar threshold values (e.g., 3.14, 3.12, 3.13). SilentWood’s node clustering algorithm clusters them, computes their weighted average as 3.131 using the formula shown in the dashed box, and updates their original threshold values to 3.131 as the representative threshold of the cluster. Now that these 3 nodes have the same threshold values, their comparison results are guaranteed to be the same. Thus, we only need to homomorphically compute and rotate the comparison result once for these 3 nodes instead of three times.

Meanwhile, updating a trained model’s thresholds to a new value could affect the model accuracy either positively or negatively. Therefore, the key challenge of node clustering is to cluster as many nodes as possible while preventing (or minimizing) the model’s accuracy loss. For this purpose, SilentWood’s node clustering introduces the following techniques: (i) clustering intensity adjustment, (ii) weighted averaging, (iii) leaf value re-optimization; and (iv) accuracy-preserving merge.

Clustering Intensity: We select the thresholds to cluster based on the learnable clustering intensity parameter s . We cluster two nodes n_i and n_j if they share the same feature name and their ratio of threshold difference is small enough to satisfy: $\frac{|n_i.threshold - n_j.threshold|}{\text{MAX}(n_i.name) - \text{MIN}(n_i.name)} < s$. Note that $\text{MAX}(n_i.name)$ and $\text{MIN}(n_i.name)$ are the maximum and minimum values of n_i ’s feature across the entire training dataset. The ideal intensity of node clustering is learnable and depends on the characteristics of each dataset.

Weighted Threshold Average: Once we construct a cluster \mathcal{C} , we update the thresholds in the cluster to their weighted average. SilentWood’s weighted average formula uses the tree weight (α) and

Algorithm 1 Accuracy-preserving merge

```

1: Input:  $\mathcal{N}$ ,  $s \triangleright$  nodes, clustering intensity
2: repeat
3:    $changed \leftarrow \text{false}$ 
4:   for  $n_i \in \mathcal{N}$  do
5:      $\mathcal{C} \leftarrow \{n \in \mathcal{N} \mid n.name = n_i.name \wedge \frac{|n.threshold - n_i.threshold|}{\text{MAX}(n_i.name) - \text{MIN}(n_i.name)} < s\}$ 
6:     if  $|\mathcal{C}| > 1$  then
7:       for  $n \in \mathcal{C}$  do
8:          $n.threshold \leftarrow \text{WeightedAverage}(\mathcal{C})$ 
9:       end for
10:       $changed \leftarrow \text{true}$ 
11:    end if
12:  end for
13: until  $\neg changed \triangleright$  stop when no more clustering occurs
14: Output:  $\mathcal{N} \triangleright$  clustered final tree nodes

```

the node weight (β). α_i and β_j refer to the contributions of tree i and the contribution of node j for computing inference results. The motivation behind the weighted average is that the more important the tree & node to which a threshold belongs, the smaller amount we change its value during the threshold update (to minimize the impact on the model accuracy). Conversely, if the tree & node to which a threshold belongs is less important, we allow a greater change in its value.

To compute α_i (i.e., the i -th tree’s weight), we sum the hit absolute leaf values of all training samples on the i -th tree as w_i , and then normalize it by computing $\alpha_i = \frac{w_i}{\sum_{k=1}^T w_k}$ (where T is the total number of trees). We compute node j ’s weight β_j as the fraction of the information gain of node j among all nodes in \mathcal{C} that belong to this tree. Using all α_i and β_j , we scale thresholds and compute the weighted average as:

$$t_{average} = \frac{\sum_{i=1}^T \alpha_i \cdot \frac{\sum\{\beta_j \cdot t_j \mid n_j \in \text{Tree}_i \wedge n_j \in \mathcal{C}\}}{\sum\{\beta_j \mid n_j \in \text{Tree}_i \wedge n_j \in \mathcal{C}\}}}{\sum_{i=1}^T \alpha_i}$$

, which is equivalent to the dashed box in Figure 3.

Leaf Value Re-optimization: After updating thresholds for a cluster \mathcal{C} , we re-optimize the leaf values (scores) while keeping the tree topology fixed. Concretely, we re-route the training samples under the updated thresholds and, for each leaf ℓ , aggregate the first-order and second-order loss derivatives with respect to the raw prediction $\hat{y}(x)$: $G_\ell = \sum_{x \in \ell} \frac{\partial}{\partial \hat{y}(x)} \mathcal{L}(y(x), \hat{y}(x))$, $H_\ell = \sum_{x \in \ell} \frac{\partial^2}{\partial \hat{y}(x)^2} \mathcal{L}(y(x), \hat{y}(x))$. We then apply a regularized Newton update to the leaf value: $v_\ell \leftarrow v_\ell - \eta \cdot \frac{G_\ell}{H_\ell + \lambda}$, where λ is the ℓ_2 regularization coefficient on leaf values and η is the learning rate. This update recalibrates the existing leaf outputs under the modified decision boundaries induced by threshold averaging.

Accuracy-preserving Merge: Once the candidate cluster \mathcal{C} ’s thresholds are weight-averaged and leaves are re-optimized, we decide whether to commit/abort it based on Algorithm 1. Basically, we evaluate the updated model on the validation set: if validation accuracy is unchanged or improved, we commit; otherwise we abort. We repeat this in an agglomerative (bottom-up) manner until no more merge-able thresholds remain (outer loop in line 4). Our evaluation (Table 7) shows that setting s as a high value does not harm the model accuracy because failed merges are aborted, anyway.

Applying Node Clustering to MPC: Node clustering reduces the number of comparisons during inference, which decreases the overall computational overhead of homomorphic operations in encrypted

protocols. Meanwhile, this technique also benefits MPC protocols because the comparison operation in an MPC setup is generally expensive. For instance, our results in Table 13 (§D) illustrate that garbled circuit-based private inference in XGBoost spends 84.1% of the total time on comparisons. Reducing the number of nodes to run MPC directly lowers this overhead, effectively reducing the total runtime of the protocol (see §D for details). To this end, node clustering is compatible with both FHE and MPC settings.

4.1.2 Path Clustering. SilentWood further reduces the number of homomorphic computations by the path clustering technique. Suppose the example where two trees have paths having the same set of threshold conditions as follows: one path's conditions along the path is $\text{sleep} > 8 \wedge \text{age} > 45$, and the other path's condition is $\text{age} > 45 \wedge \text{sleep} > 8$. The only difference in these two paths is the order of their nodes. Therefore, their aggregate leaf conditions are the same because their results are insensitive to the order of node conditions. This implies that their SumPath (or MultiplyPath) values will also be the same; therefore, the server only needs to compute one SumPath (or MultiplyPath) value for each path having a unique set of unordered node conditions. SilentWood regards the path evaluation results of any two paths as being the same if they have the same set of (*feature, threshold*) pairs comprising their paths. Unlike node clustering which clusters the thresholds having similar values, path clustering clusters those paths that have exactly the same (unordered) set of node conditions along their paths and thus has no impact on model accuracy.

4.2 Blind Code Conversion (BCC)

In gradient boosting, computing the final score requires homomorphically summing the leaf values of true paths in a computationally efficient manner. But as explained in C2 in §3, existing private path evaluation methods fail: in the case of SumPath (e.g., RCC-PDTE), its outputs (0 for true, and a random non-zero value for false) cannot arithmetically derive final leaf scores. MultiplyPath (e.g., Sorting-Hat) can do this, but at the cost of high overhead from multiplication chains that grow polynomially with tree depth.

To solve this dilemma, SilentWood introduces a practical two-party blind code conversion (BCC) protocol. The server sends an intermediate ciphertext containing padded, uniformly shuffled SumPath values to the client. Then, the client decrypts it, flips 0s to 1s and non-zero random values to 0s, re-encrypts, and returns them. Now, only true SumPath entries are 1s, and false ones are 0s. Thus, so the server can compute true leaf scores via a single homomorphic multiplication with the plaintext leaf array aligned with the SumPath values. Since we use SumPaths, the path evaluation overhead remains almost constant as tree depth grows. Security-wise, BCC ensures that neither the server nor the client learns anything about the original SumPath values in the intermediate ciphertext.

Figure 4 shows an example of XGBoost score computation based on the BCC protocol. Initially, the server has a list of SumPath ciphertexts, each of which contains a distinct SumPath in slot index 0 and zero values in other slots. In step 1, the server extracts only encrypted SumPaths, randomly rotates each of them, and merges them into a new array \bar{u} . The output of step 1 is $\langle\langle \bar{u} \rangle\rangle$ (where $\langle\langle \cdot \rangle\rangle$ denotes encryption). In step 2, the server homomorphically adds dummy

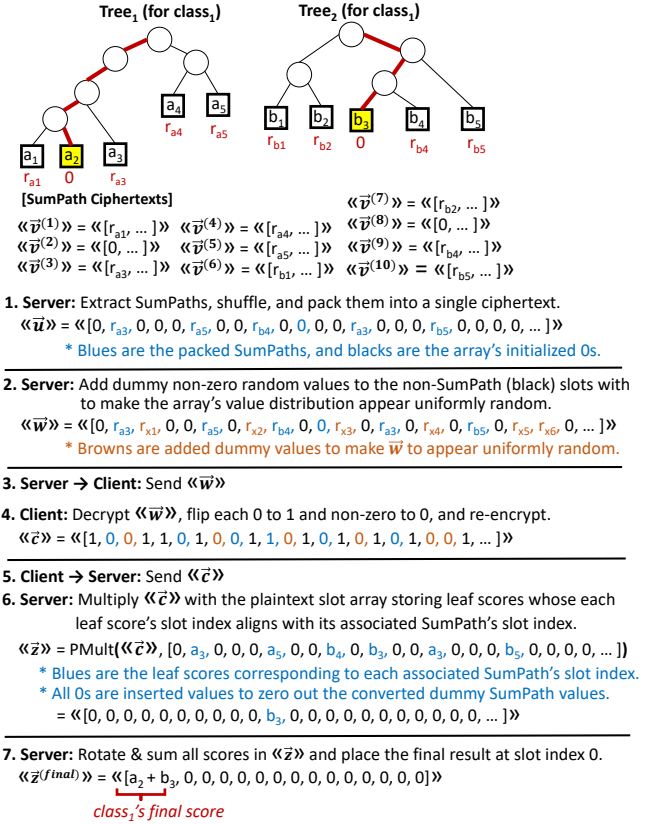


Figure 4: An example of BCC for XGBoost scoring.

values to \bar{u} to make the ratio between the zeros and non-zeros uniform (1:1 in Figure 4's example) and randomly ordered. This ratio is a fixed hyperparameter of the protocol. In step 3, the server sends the ciphertext to the client. In step 4, the client decrypts it, flips 0s to 1s and non-zeros to 0s, re-encrypts them, and sends them back to the server. During this process, the client learns nothing about the real SumPath values because the decrypted slot array is indistinguishable from a uniformly random array comprising zeros and non-zeros. The server also learns nothing about the SumPath values because they always remain encrypted when handled by the server. In step 5, the server receives the ciphertext containing client-converted values. In step 6, the server homomorphically multiplies the ciphertext by the server's plaintext array that encodes the leaf values (scores), where each array slot's leaf value aligns with its associated SumPath's slot index. Thus, when we multiply this array with the client-returned ciphertext, the leaf values for false SumPaths and dummy values are masked to 0, while those for true SumPaths remain. In step 7, the server sums all per-tree scores according to the class by rotating and adding the slot values to compute the final score for each class. Finally, the server compactly packs all final class scores into $\langle\langle \bar{z}^{(final)} \rangle\rangle$ and sends them to the client. In the case of binary classification, a single final score is returned to the client, and whether this score is positive or negative indicates the binary classification result. In the case of multi-class classification, the highest class score is regarded as the inferred class.

Notations	
N	: The number of plaintext slots in an RLWE ciphertext
Z_p	: $\{0, \dots, p-1\}$, the plaintext space
\mathcal{U}_p	: A custom conversion table which defines the mapping of each plaintext value $\{0, \dots, p-1\}$ to some $\{u_0, u_1, \dots, u_{p-1}\}$
f	: A frequency distribution as the protocol's hyperparameter
$\vec{v}^{(i)}$: An array whose slot index 0 stores the i -th SumPath value
\vec{u}	: An intermediate array that stores shuffled SumPath values
\vec{w}	: An array that appears to store values randomly sampled from the distribution f , some of which are real SumPaths
\vec{c}	: The client converts \vec{w} into \vec{c} according to table \mathcal{U}_p
$\langle\langle \vec{v}^{(i)} \rangle\rangle$: A ciphertext encrypting $\vec{v}^{(i)}$ \triangleright the same applies to: $\vec{u}, \vec{w}, \vec{c}$
Protocol	
Input	: $\{\langle\langle \vec{v}^{(i)} \rangle\rangle\}_{i=1}^\ell \triangleright$ a list of ℓ ciphertexts storing all ℓ SumPaths
Server	: 1) Randomly rotate each $\{\langle\langle \vec{v}^{(i)} \rangle\rangle\}_{i=1}^\ell$ and merge them as $\langle\langle \vec{u} \rangle\rangle$. 2) Create a random dummy array \vec{d} such that the values of the array $\vec{u} + \vec{d}$ appears to have distribution f . 3) $\langle\langle \vec{w} \rangle\rangle \leftarrow \text{PAdd}(\langle\langle \vec{u} \rangle\rangle, \text{Encode}(\vec{d}))$.
S\rightarrowC	: Send $\langle\langle \vec{w} \rangle\rangle$ and \mathcal{U}_p .
Client	: 1) Decrypt $\langle\langle \vec{w} \rangle\rangle$ to \vec{w} . 2) Create \vec{c} by converting each value in \vec{w} according to \mathcal{U}_p . 3) Encrypt \vec{c} to $\langle\langle \vec{c} \rangle\rangle$.
C\rightarrowS	: Send $\langle\langle \vec{c} \rangle\rangle$.
Output	: $\langle\langle \vec{c} \rangle\rangle$

Table 1: The blind code conversion (BCC) protocol

In Figure 4, steps 1 ~ 5 comprise the generic BCC protocol (which we formally describe in Table 1), whereas steps 6 ~ 7 involve application-specific score computation for XGBoost.

4.2.1 Blind Shuffling. In step 1~2 of the BCC protocol in Figure 4 (which corresponds to step 1~3 in Table 1), the server effectively pads and shuffles the SumPath slots to create a uniformly random distribution comprising zeros and non-zeros in a 1:1 ratio (or the distribution f defined by the hyperparameter). Since this shuffling is to be done homomorphically, computational efficiency is critical.

Algorithm 2 describes SilentWood's shuffling process in detail. The inputs are: (1) T , the number of trees; (2) $\{\langle\langle \vec{v}^{(i)} \rangle\rangle\}_{i=1}^\ell$, a list of ciphertexts, each of which stores a SumPath at slot index 0 and zero in other indices; and (3) $\{s_i\}_{i=1}^\ell$, a list of leaf scores. We generate a random permutation plan $\vec{\sigma}$ (line 2), rotate SumPaths in ciphertexts according to it, and add them to an empty ciphertext (line 4~6). We also generate dummy SumPaths and place each of them into the permuted position in a new array (line 9~11). Finally, we merge randomly permuted real SumPaths and dummy SumPaths to obtain the final ciphertext, which stores uniformly shuffled zeros and non-zero random values with a ratio of 1:1 (line 13). In addition, we prepare an array of leaf scores, whose each slot index is aligned with its corresponding permuted real SumPath's index (lines 4, 7).

Once the client returns to the server a ciphertext containing converted values (i.e., $0 \mapsto 1$, non-zero $\mapsto 0$), the server computes the final inference score as in Algorithm 3. The server multiplies the returned ciphertext by the array of leaf scores to filter out only the scores of true SumPaths (line 2). Note that the server knows the exact slot index of each real SumPath value, even after shuffling them (although it does not know their plaintext contents) because the server knows the shuffling sequences. So, the server can appropriately generate the leaf value plaintext to homomorphically multiply by the converted ciphertext $\langle\langle \vec{c} \rangle\rangle$ for final score aggregation. Finally, the server aggregates the filtered scores and stores them at slot index 0 (line 3~9).

Algorithm 2 Blind Shuffling (Server's step 1~3 in Table 1)

```

1: Input:  $T, \{\langle\langle \vec{v}^{(i)} \rangle\rangle\}_{i=1}^\ell, \{s_i\}_{i=1}^\ell$ 
    $\triangleright$  total number of trees, encrypted SumPaths, plain leaf scores
2:  $\vec{\sigma} \leftarrow \text{genDist}(f) \triangleright$  random permutation offsets for  $N$  slots having distribution  $f$ 
3:  $\vec{x} \leftarrow 0 \triangleright$  a slot array to store leaf scores
4:  $\langle\langle \vec{u} \rangle\rangle \leftarrow \langle\langle [0, 0, \dots, 0] \rangle\rangle \triangleright$  A ciphertext to store shuffled SumPaths
5: for  $i$  in  $\{1, 2, \dots, \ell\}$  do  $\triangleright$  permute each  $i$ -th SumPath
6:    $\langle\langle \vec{u} \rangle\rangle \leftarrow \text{CAdd}(\langle\langle \vec{u} \rangle\rangle, \text{Rotate}(\langle\langle \vec{v}^{(i)} \rangle\rangle, \sigma_i))$ 
7:    $x_{\sigma_i} \leftarrow s_i \triangleright$  Also, store the slot-aligned leaf score
8: end for
9:  $\vec{d} \leftarrow 0 \triangleright$  a slot array to store dummy SumPaths
10: for  $i$  in  $\{\ell + 1, \dots, N - (f_{\text{zero}} - T)\}$  do  $\triangleright f_{\text{zero}}$ : frequency of zeros
11:    $d_{\sigma_i} \leftarrow \text{rand}() \triangleright$  permute dummy non-zero SumPaths
12: end for
13:  $\langle\langle \vec{w} \rangle\rangle \leftarrow \text{PAdd}(\langle\langle \vec{u} \rangle\rangle, \text{Encode}(\vec{d})) \triangleright$  merge the dummy SumPaths
14: Output:  $\langle\langle \vec{w} \rangle\rangle, \vec{x}$ 
    $\triangleright$  uniformly padded and shuffled SumPaths, slot-aligned leaf scores

```

Algorithm 3 Blind Score Aggregation (steps after Table 1)

```

1: Input:  $\langle\langle \vec{c} \rangle\rangle, \vec{x} \triangleright$  client-converted SumPaths, slot-aligned scores
2:  $\langle\langle \vec{z} \rangle\rangle \leftarrow \text{PMult}(\langle\langle \vec{c} \rangle\rangle, \text{Encode}(\vec{x})) \triangleright$  zero out scores of false paths
3: for  $n$  in  $\{\log_2 N, (\log_2 N) - 1, \dots, 2, 1\}$  do
4:    $\vec{m}^{(1)} \leftarrow [ \underbrace{1, \dots, 1}_{2^{n-1} \text{ slots}}, \underbrace{0, \dots, 0}_{2^{n-1} \text{ slots}}, \underbrace{0, \dots, 0}_{N - 2^n \text{ slots}} ] \triangleright$  Filter for the 1st  $2^{n-1}$  slots
5:    $\vec{m}^{(2)} \leftarrow [ \underbrace{0, \dots, 0}_{2^{n-1} \text{ slots}}, \underbrace{1, \dots, 1}_{2^{n-1} \text{ slots}}, \underbrace{0, \dots, 0}_{N - 2^n \text{ slots}} ] \triangleright$  Filter for the 2nd  $2^{n-1}$  slots
6:    $\langle\langle \vec{z}^{(1)} \rangle\rangle = \text{PMult}(\langle\langle \vec{z} \rangle\rangle, \text{Encode}(\vec{m}^{(1)}))$ 
7:    $\langle\langle \vec{z}^{(2)} \rangle\rangle = \text{PMult}(\langle\langle \vec{z} \rangle\rangle, \text{Encode}(\vec{m}^{(2)}))$ 
8:    $\langle\langle \vec{z} \rangle\rangle = \text{CAdd}(\langle\langle \vec{z}^{(1)} \rangle\rangle, \text{Rotate}(\langle\langle \vec{z}^{(2)} \rangle\rangle, 2^{n-1})) \triangleright$  align and add up
9: end for
10: Output:  $\langle\langle \vec{z} \rangle\rangle \triangleright$  slot index 0 contains the final aggregated score

```

The computational benefit of Algorithm 2 and 3 is that its critical circuit depth is affected only by $O(\log l)$ CAdd operations (line 6), while all Rotate operations can run in parallel, consuming 1 circuit depth. Thus, the algorithm's accumulating noise remains almost unaffected even if the tree sizes grow (i.e., depths or paths), because the computation overhead of CAdd in FHE is small. Further, the Rotate permutations of ℓ SumPaths (lines 6 in Algorithm 2) can run in parallel with the maximum ℓ parallelism level, which can take full advantage of multi-core CPUs or GPUs. See Table 11 (in §B.1) for further details on BCC's time complexity and its comparison to that based on MultiplyPath.

In the case of a very large model, if the total number of SumPaths exceeds N and does not fit in a single ciphertext, Algorithm 2 and 3 can run on multiple ciphertexts in parallel to handle any required number of SumPaths.

Throughout SilentWood's entire private inference protocol, the only information the client learns is that the total number of tree paths in the server's model is capped at some multiple of N , which is fixed as a hyperparameter (e.g., 16384 if RLWE's polynomial degree $N = 2^{14}$).

Extension to AdaBoost: Figure 4's XGBoost score computation can be transformed into AdaBoost score computation by replacing each leaf plaintext with $+\omega$ or $-\omega$, where the sign indicates the leaf's binary class label and ω is the weight of the tree it belongs to. As only the scalar values of the leaf plaintext need to be modified to turn the XGBoost into AdaBoost score computation, the total computation time and complexity are identical to those of the XGBoost protocol.

BCC can be used for general FHE applications where the true frequency distribution of values for programmable bootstrapping in

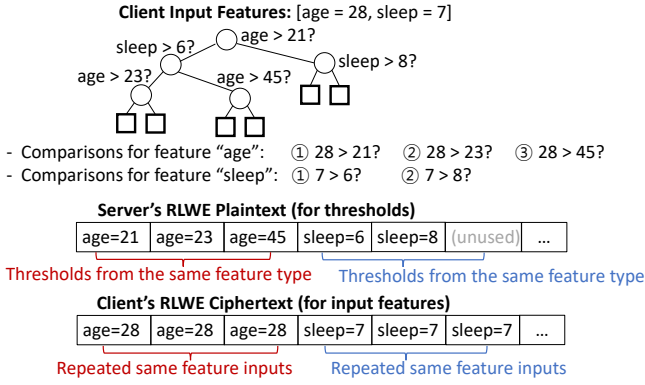


Figure 5: An example of repetitive data encoding

a target ciphertext is the server's private information to be hidden from the client (e.g., the number of zero SumPaths, since it equals the total number of trees in XGBoost).

§B provides a formal analysis of the BCC protocol.

4.3 Ciphertext Compression

As discussed in C3 in §3, another challenge in private decision forest evaluation is reducing the communication overhead caused by verbose bit-wise data encryption. In the example of RCC-PDTE [3], the largest communication overhead occurs when the client sends the encrypted feature inputs to the server, which accounts for more than 95% of the total communication size [3]. Meanwhile, the overhead of the final ciphertext, storing the server's inference result, accounts for less than 5%. Therefore, it is critical to reduce the size of the client's initial query ciphertexts.

Figure 5 is an example showing how PDTE generally uses repetitive data encoding: the server's tree has 3 nodes conditioned on the *age* feature (each threshold is 21, 23, and 45) and 2 nodes conditioned on the *sleep* feature (each threshold is 6 and 8). The server homomorphically compares these threshold values against the client's encrypted *age=28* and *sleep=7* input feature values in a SIMD manner. Since the server has 3 distinct threshold values for *age* and 2 distinct threshold values for *sleep*, the client encodes its *age=28* and *sleep=7* values repetitively 3 times (capping to the server's maximum number of comparisons for any same feature name). While such repetitive data encoding enables efficient SIMD comparisons, this repetition wastes ciphertext slot utility.

To resolve this issue, SilentWood designs the ciphertext compression protocol, which works as follows: (1) the client removes repetitive data encoding before encryption and generates size-reduced compact ciphertexts; (2) once the server receives them, it *homomorphically* decompresses them by restoring the originally intended repetitions of data encoding. Figure 6 shows an example of ciphertext compression. In FHE-based private protocols, when a client CW-encodes feature data, s/he has to create as many ciphertexts as the number of feature data bits (M in Figure 6's example), where each ciphertext repetitively encodes each feature's same bit 3 times (to help the server-side SIMD operation). On the other hand, using SilentWood's ciphertext compression, the client removes these repetitions of data before encrypting them, which results in 2 empty slots for each feature bit storage in the ciphertext. Therefore, the

Algorithm 4 Ciphertext compression

```

1: Input: dataArrList, dataInitIndices, gapList, repetition ▷ data array list, each data's
   start index, repetitive encoding gaps, repetitions
2: cDataArrList ← [] ▷ compressed array list
3: cDataArr ← [] ▷ compressed single array
4: dataArrCount ← 0 ▷ current data array count
5: cDataArrCount ← 0 ▷ current compressed array count
6: for dataArr ∈ dataArrList do ▷ this loop compresses all data
7:   repeatRound ← dataArrCount mod repetition
8:   for {data, initIndex} ∈ {dataArr, dataInitIndices} do
9:     targetIndex ← initIndex + gapList[repeatRound]
10:    cDataArr[targetIndex] ← data ▷ compactly position the data
11:   end for
12:   dataArrCount ← dataArrCount + 1
13:   if repeatRound + 1 = repetition then ▷ current plaintext array full?
14:     cDataArrList.append(cDataArr)
15:     cDataArr ← [] ▷ prepare a new plaintext array
16:   end if
17: end for
18: encCDataArrList ← []
19: for cDataArr ∈ cDataArrList do ▷ encrypt all plaintext arrays
20:   encCDataArr ← Encrypt(Encode(cDataArr), sk) ▷ notations §2.2
21:   encCDataArrList.append(encCDataArr)
22: end for
23: Output: encCDataArrList
    
```

client can store the bits of other digits of data in this available extra space. Applying this compact data encoding, the total required number of ciphertexts reduces from M to $\frac{M}{3}$. Once the server receives these compressed ciphertexts, it homomorphically performs a reverse operation of what the client did, effectively decompressing and restoring the originally intended data encoding (i.e., 3 repetitions of feature bits).

Algorithm 4 generalizes the ciphertext compression algorithm, whose inputs are the following four: (1) the list of plaintext data arrays (*dataArrList*); (2) the list of each unique data's initial slot index (*dataInitIndices*); (3) the gap offsets between each repetitive data encoding (*gapList*); and (4) the number of intended data repetitions in each ciphertext (*repetition*). One important requirement for the ciphertext compression algorithm is that all distinct data elements to be repeated in each round of repetition should have the same gap to their next round of data repetition so that the server can restore the repetitions of all distinct data elements homogeneously in a SIMD manner (e.g., the repetition of both the *age* and *sleep* feature data is recovered simultaneously). The ciphertext decompression algorithm is a reverse operation of Algorithm 4 (i.e., Algorithm 5 in §C), which is implemented by a series of homomorphic rotation, multiplication, and addition operations. SilentWood's ciphertext decompression is *homomorphic* decompression: unlike regular plaintext data compression algorithms (e.g., LZ77, LZW, Huffman coding) whose decompression process requires (or leaks) information about the compressed data (e.g., token dictionary or code table), SilentWood's ciphertext decompression process does not leak any information of the underlying plaintext values to the decompressing entity.

5 Evaluation

Implementation: We implemented SilentWood in C++ (5518 lines), which includes the BCC protocol, computation clustering, and ciphertext compression techniques. We implemented Python code (737 lines) that trains XGBoost models with node clustering. We trained the model based on the dataset ratio of training : validation : testing as 6:2:2. For FHE computation, we used the SEAL library [14]

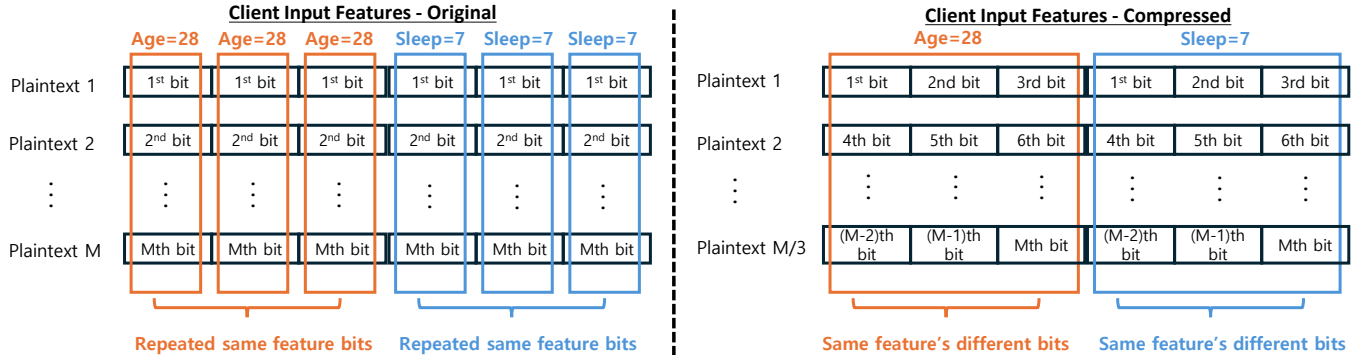


Figure 6: An example of ciphertext compression

	Spam	Steel	Breast	Heart	Defect	Bank	PenDigits	Ailerons	Credit	Satellite	Elevators	Telescope	MFeat
Features	57	33	30	13	32	21	16	40	30	36	18	11	64
Classes	2	2	2	5	2	2	2	2	2	2	2	2	10
Samples	4,601	1,941	569	294	8,191	10,885	10,992	14,750	14,143	5,100	16,599	19,020	2,000

Table 2: Specification of benchmarks

Benchmark	MPC		CPU-FHE				GPU-FHE					
	SoK-GGG		Zama	Baseline		SilentWood		Zama	Baseline		SilentWood	
	16-bit	32-bit	14-bit	16-bit	32-bit	16-bit	32-bit	14-bit	16-bit	32-bit	16-bit	32-bit
Spam	5.98s	5.95s	72.68s	153.68s	162.53s	3.82s	5.26s	47.42s	N/A	N/A	1.65s	2.27s
Steel	5.41s	5.56s	18.01s	37.24s	38.32s	1.81s	1.98s	10.57s	3.86s	5.62s	1.04s	1.21s
Breast	5.24s	2.69s	12.32s	20.62s	28.27s	1.57s	1.81s	9.08s	2.71s	4.85s	1.02s	1.08s
Heart	23.52s	23.26s	96.08s	174.19s	188.32s	3.76s	4.11s	75.65s	N/A	N/A	1.75s	1.95s
Defect	6.38s	6.39s	145.05s	336.04s	349.23s	6.92s	8.38s	83.66s	N/A	N/A	2.71s	3.33s
Bank	6.39s	6.45s	223.03s	436.02s	458.97s	9.39s	10.95s	151.14s	N/A	N/A	4.24s	4.16s
PenDigits	5.53s	5.47s	62.12s	71.76s	72.28s	2.17s	2.56s	49.68s	5.70s	7.53s	1.13s	1.31s
Ailerons	6.53s	6.56s	N/A	370.20s	392.15s	7.73s	10.08s	N/A	N/A	N/A	2.96s	3.97s
Credit	5.31s	5.20s	5.99s	17.51s	20.89s	1.52s	1.76s	5.55s	2.66s	4.52s	1.00s	1.08s
Satellite	4.03s	5.30s	14.49s	30.24s	36.08s	1.63s	1.91s	10.57s	3.50s	5.40s	1.05s	1.20s
Elevators	6.33s	6.24s	289.13s	427.75s	442.75s	8.39s	10.48s	149.87s	N/A	N/A	3.34s	4.07s
Telescope	4.85s	4.88s	181.88s	7.19s	9.20s	1.33s	1.57s	108.58s	1.94s	3.78s	0.89s	1.04s
MFeat	41.08s	41.57s	147.99s	301.05s	315.66s	6.81s	9.53s	169.62s	N/A	N/A	2.77s	3.86s
AVG.	9.73s	9.88s	113.73s	185.58s	191.19s	4.37s	5.41s	67.03s	3.40s	5.28s	1.97s	2.35s
SilentWood's Speedup	2.2x	1.8x	27.8x	42.5x	32.7x	-	-	34.0x	3.3x	4.6x	-	-

Table 3: Comparing inference time over various data bit-lengths (14 bits, 16 bits, and 32 bits) w/o GPU support. N/A denotes GPU (or RAM) failure due to large-memory-consuming FHE parameters.

Bench.	Baseline	Baseline+B	Baseline+B+K	Baseline+B+K+C (SilentWood)
Spam	162.53s	9.89s	6.59s	5.26s
Steel	38.32s	3.06s	2.26s	1.98s
Breast	28.27s	2.84s	2.21s	1.81s
Heart	188.32s	8.58s	4.06s	4.11s
Defect	349.23s	15.68s	9.43s	8.38s
Bank	458.97s	16.20s	16.20s	10.95s
PenDigits	72.28s	3.66s	3.66s	2.56s
Ailerons	392.15s	19.74s	12.24s	10.08s
Credit	20.89s	2.18s	1.79s	1.76s
Satellite	36.08s	2.52s	2.27s	1.91s
Elevators	442.75s	21.62s	11.37s	10.48s
Telescope	9.20s	1.92s	1.74s	1.57s
MFeat	315.66s	1.74s	1.74s	9.53s
AVG.	191.19s	9.69s	6.34s	5.41s
Speedup against Baseline		19.7x	30.3x	32.7x

Table 4: Speedup of SilentWood's each technique.

for CPU-based FHE and extended its code with the techniques of PhantomFHE [50] for GPU-based FHE.

Setup: We used i9-14900K 24-core CPU, 168GB RAM, and RTX 4090 GPU. To train and evaluate XGBoost, we used 13 UCI datasets [41], whose numbers of features, classes, and sample sizes are summarized in Table 2. We compared the performance of the four systems: XGBoost based on Zama's Concrete ML (based on the TFHE-rs library) [53], SoK-GGG (an MPC protocol based on a 2-party garbled circuit) [35], Baseline (RCC-PDTE [3] with MultiplyPath [19]), and SilentWood. The default round-trip time (RTT) was 50ms, the default number of trees was 100, the default maximum tree depth was 7, and the default intensity of node clustering was 0.2. We measured inference time, inference accuracy, and ciphertext size. We also conducted an ablation study for our proposed techniques, over various tree counts (100, 200, 300), maximum depths (7, 11, 15), and RTTs (0ms, 50ms, 100ms) by using netem [42].

Summary of Results: When using CPU-FHE, SilentWood's end-to-end inference time (with an RTT of 50ms) is faster than Baseline

Bench.	Inference Time			Model Accuracy			Inference Time			Model Accuracy		
	100T	200T	300T	100T	200T	300T	7D	11D	15D	7D	11D	15D
Spam	3.82s	5.49s	6.68s	0.94	0.94	0.94	3.82s	4.42s	4.92s	0.94	0.94	0.94
Steel	1.81s	2.33s	2.69s	1.00	1.00	1.00	1.81s	1.79s	1.73s	1.00	1.00	1.00
Breast	1.57s	1.69s	1.82s	0.96	0.96	0.96	1.57s	1.45s	1.46s	0.96	0.96	0.96
Heart	3.76s	4.97s	6.67s	0.63	0.59	0.61	3.76s	3.18s	3.86s	0.63	0.62	0.62
Defect	6.92s	12.73s	14.39s	0.79	0.81	0.80	6.92s	11.23s	16.38s	0.79	0.81	0.80
Bank	9.39s	10.66s	12.42s	0.79	0.80	0.79	9.39s	12.47s	12.51s	0.79	0.79	0.79
Pendigits	2.17s	2.33s	2.40s	0.99	1.00	1.00	2.17s	2.22s	2.01s	0.99	1.00	1.00
Ailerons	7.73s	10.59s	12.34s	0.87	0.88	0.88	7.73s	11.99s	15.12s	0.87	0.87	0.87
Credit	1.51s	1.59s	1.58s	1.00	1.00	1.00	1.51s	1.45s	1.46s	1.00	1.00	1.00
Satellite	1.63s	1.69s	1.87s	0.99	0.99	0.99	1.63s	1.62s	1.57s	0.99	0.99	0.99
Elevators	8.39s	10.82s	14.49s	0.78	0.78	0.78	8.39s	15.38s	18.02s	0.78	0.78	0.78
Telescope	1.33s	1.41s	1.54s	1.00	1.00	1.00	1.33s	1.27s	1.24s	1.00	1.00	1.00
MFeat	6.81s	6.68s	7.55s	0.91	0.93	0.93	6.81s	6.13s	6.19s	0.91	0.91	0.91
AVG.	4.37s	5.61s	6.65s	0.90	0.90	0.90	4.37s	5.74s	6.65s	0.90	0.90	0.90

Table 5: Inference time over various numbers of trees (100T~300T) and maximum tree depths (7D~15D).

by 32.7x, faster than Zama by 27.8x, and faster than SoK-GGG by 2.2x. When using GPU-FHE, SilentWood is faster than Baseline by 4.6x, faster than Zama by 34.0x, and faster than SoK-GGG by 3.6x. SilentWood is faster than SoK-GGG on average even when RTT is 0 ms, and the speedup grows to 2.94x when RTT is 200 ms. Compared to Baseline, SilentWood reduces the server-client communication size to roughly 1/5 on average.

5.1 End-to-end Inference Time

We evaluated end-to-end inference time with an RTT of 50ms (including the server and client’s encoding/decoding, encryption/decryption, and homomorphic operations) for the cases where the feature and threshold bit sizes are 16 bits and 32 bits (quantized), respectively. The results are illustrated in Table 3. We tested only 14 bits for Zama because its framework supports a maximum 14 bit data length. We evaluated the cases w/o GPU. Without a GPU, Baseline’s average computation time is 185.58 s (16 bits) and 191.19 s (32 bits), while Zama’s average time is 113.73 s (14 bits). In contrast, SilentWood’s time is 4.37 s (16 bits) and 5.41 s (32 bits). When using a GPU, Baseline’s average computation time is 3.40s (16 bits) and 5.28s (32 bits), and Zama’s average time is 67.03s (14 bits), whereas SilentWood’s average time is 1.97s (16 bits) and 2.35s (32 bits).

The FHE-based systems (Zama, Baseline, SilentWood) required a longer computation time for the 32-bit data size, whereas for MPC (SoK-GGG) was less-sensitive to the data bit-length but more sensitive to depth. For the breast dataset, SoK-GGG’s runtime is shorter for 32-bit than for 16-bit because the trained 32-bit model had shallower tree depths.

5.2 Ablation Study and Model Resizing

In Table 4, we evaluated the effectiveness of SilentWood’s each technique: Baseline plus BCC (denoted as Baseline + B), plus computation clustering (denoted as Baseline + B + K), and plus ciphertext compression (denoted as Baseline + B + K + C). We used CPU-FHE and an RTT of 50ms for these evaluations. Table 4 illustrates the speedup contributions of SilentWood’s each technique: BCC’s contribution was the largest for the speedup (about 19.7x on average); computation clustering was next (1.54x), and ciphertext compression was last (about 1.08x). Later in §5.4, our results indicate that

the speedup by ciphertext compression grows as the RTT increases from 50ms to 100ms and 200ms (Table 10).

Table 5 shows the average inference time across various numbers of trees (100 ~ 300). For all four versions, the average computation time roughly increased linearly with the number of trees, as their number of rotations to handle SumPath also increased linearly. In Table 5, we also measured the change in inference time across various maximum tree depths (7, 11, 15). For all four versions, the average inference time increased with depth (not due to BCC, but due to SumPath computation). The increase between 11 and 15 is relatively bigger than that between 7 and 11.

Model Accuracy: Table 5 also illustrates the accuracy of each trained XGBoost model (measured using the testing datasets) across various numbers of trees and maximum tree depths. Note that these measured model accuracies are affected only by the training parameters, not by the optimization techniques of SilentWood. The average model accuracy of all benchmarks was 0.9 for all numbers of trees (100~300) and all maximum tree depths (7~15). This implies that 100 trees with a maximum depth of 7 are generally a sufficient setup to achieve the best accuracy for private XGBoost inference.

5.3 Further Analysis on Each Technique

We more closely analyzed the effectiveness of SilentWood’s each of three techniques: computation clustering, BCC, and ciphertext compression.

Node Clustering: Figure 7 shows the number of node clusters across various clustering intensities s (0.0 ~ 1.0), where two nodes n_i and n_j are co-clustered if $\frac{|n_i.val - n_j.val|}{\max(n_i.name) - \min(n_i.name)} < s$. The success of clustering gradually decreased as we increased the intensity s . For example, when intensity $s = 0.2$, on average, 2,388 nodes in XGBoost were clustered into 46 node clusters (i.e., $\frac{46}{2388} = 51.9x$ node reduction rate). While the greater clustering intensity provided a higher opportunity for node clustering, the effectiveness of clustering (i.e., node reduction rate) did not increase further when s was greater than 0.4. Table 7 shows that the average model accuracy across all benchmarks (measured by the testing datasets) does not drop below 0.90 even with high s values, because after each round of node clustering, we validate (by using the validation datasets) the inference accuracy of the updated XGBoost model and abort the change if the model accuracy decreases. This way, we preserve model correctness even under aggressive clustering.

Table 6 shows the statistics for the number of eliminated paths by path clustering. On average, the technique eliminated 21.48% of paths in a given model. Path clustering is effective if a target model has a large number of tree paths having the same set of un-ordered path conditions. For example, the Heart dataset’s XGBoost model has 3084 total tree paths, of which 45.1% have overlaps in path conditions. On the other hand, the Elevator benchmark did not gain much benefit from this technique because it does not have much overlap in path conditions.

Table 14 in §D shows model accuracy, clustering efficiency, and merge abortion rate across various validation set sizes (5%~35%). A small validation set (5%) leads to unstable accuracy, which improves and stabilizes as its size increases to 20%. At 35%, the test-set size

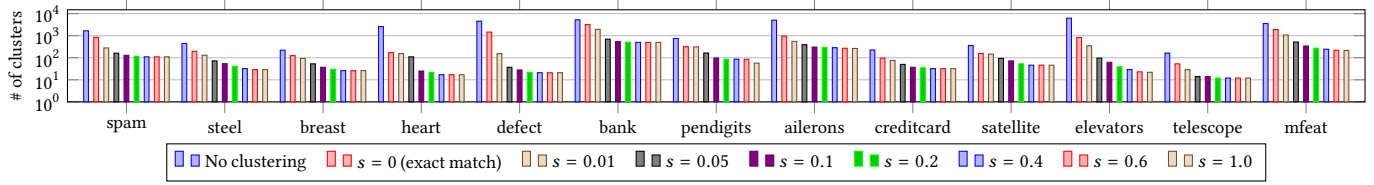


Figure 7: The number of node clusters across various node clustering intensities.

	Spam	Steel	Breast	Heart	Defect	Bank	PenDigits	Ailerons	Credit	Satellite	Elevators	Telescope	MFeat
Original Paths	1848	538	239	3084	4287	5222	823	5249	263	466	6395	239	4437
Clustered Paths	46	173	61	1403	34	0	64	10	70	104	6	226	950
% of Eliminated Paths	2.5%	32.1%	25.5%	45.5%	0.8%	0.0%	7.8%	0.2%	26.7%	22.3%	0.1%	94.4%	21.4%

Table 6: The number of redundant paths eliminated by path clustering.

	s = 0	s = 0.01	s = 0.05	s = 0.1	0.2	0.4	0.6	1
Spam	0.94	0.93	0.93	0.93	0.93	0.92	0.92	0.92
Steel	1.00	1.00	1.00	1.00	1.00	1.00	1.00	1.00
Breast	0.67	0.67	0.66	0.66	0.66	0.64	0.59	0.59
Heart	0.74	0.8	0.81	0.81	0.81	0.81	0.81	0.81
Defect	0.82	0.82	0.82	0.82	0.8	0.81	0.81	0.81
Bank	0.99	0.99	0.99	0.99	0.99	0.99	0.99	0.99
PenDigits	1.00	1.00	0.99	0.99	0.99	0.99	0.99	0.99
Ailerons	0.88	0.88	0.88	0.88	0.88	0.88	0.88	0.88
Credit	1.00	1.00	1.00	1.00	1.00	1.00	1.00	1.00
Satellite	0.99	0.99	0.99	0.99	0.99	0.99	0.99	0.99
Elevators	0.8	0.8	0.81	0.82	0.8	0.81	0.81	0.81
Telescope	1.00	1.00	1.00	1.00	1.00	1.00	1.00	1.00
MFeat	0.94	0.94	0.94	0.94	0.94	0.94	0.94	0.94
AVG.	0.90	0.90	0.90	0.90	0.90	0.90	0.90	0.90

Table 7: Model accuracy for various node clustering intensities

s

Bench.	SoK-GGG		Baseline + B + K		Baseline + B + K + C	
	16-bit	32-bit	16-bit	32-bit	16-bit	32-bit
Spam	181.2MB	182.4MB	26.7MB	85.7MB	5.8MB	22.8MB
Steel	35.0MB	36.3MB	26.7MB	85.7MB	4.5MB	16.3MB
Breast	18.3MB	9.8MB	26.7MB	85.7MB	4.5MB	12.3MB
Heart	219.4MB	208.8MB	26.7MB	85.7MB	3.2MB	7.1MB
Defect	324.9MB	322.5MB	26.7MB	85.7MB	3.4MB	10.0MB
Bank	401.6MB	381.2MB	26.7MB	85.7MB	4.7MB	17.5MB
Pendigits	64.8MB	66.6MB	26.7MB	85.7MB	3.2MB	8.4MB
Ailerons	359.4MB	358.5MB	26.7MB	85.7MB	4.7MB	16.5MB
Credit	17.6MB	13.5MB	26.7MB	85.7MB	4.5MB	12.3MB
Satellite	27.5MB	30.6MB	46.4MB	85.7MB	4.5MB	16.3MB
Elevators	401.9MB	390.8MB	26.7MB	85.7MB	3.4MB	8.7MB
Telescope	12.6MB	12.1MB	26.7MB	85.7MB	3.2MB	5.8MB
MFeat	346.5MB	341.5MB	26.7MB	85.7MB	7.1MB	43.8MB
AVG.	185.5MB	180.8MB	29.79MB	85.75MB	4.34MB	15.12MB

Table 8: Communication cost (i.e., exchanged data) between the server and client over various feature bit-lengths

drops too much, causing instability in test accuracy. As the validation-set size increases, clustering efficiency declines, and the abortion rate increases, which is natural. Our default (20% validation set, 20% test set) balances these factors effectively.

Ciphertext Compression: Table 8 shows the total size of data exchanged between the server and client during XGBoost inference,

Bench.	Cipher Decompression		BCC Computation	
	16-bit	32-bit	16-bit	32-bit
Spam	80ms	102ms	1608ms	1629ms
Steel	150ms	189ms	717ms	711ms
Breast	126ms	207ms	453ms	429ms
Heart	205ms	310ms	2314ms	2358ms
Defect	149ms	250ms	4248ms	4454ms
Bank	145ms	174ms	4713ms	4717ms
Pendigits	156ms	351ms	833ms	832ms
Ailerons	131ms	180ms	4223ms	4495ms
Credit	111ms	194ms	379ms	380ms
Satellite	112ms	178ms	498ms	518ms
Elevators	176ms	361ms	5916ms	6081ms
Telescope	209ms	412ms	335ms	367ms
MFeat	90ms	24ms	3433ms	3733ms
AVG.	142ms	226ms	2282ms	2362ms

Table 9: The computation overhead of ciphertext decompression and BCC.

where Baseline + B + K + C and Baseline + B + K are SilentWood w/o ciphertext compression. Generally, SilentWood’s ciphertext sizes were much smaller than those of SoK-GGG’s. For SilentWood w/o compression, the exchanged ciphertext size increased with the feature data size. Without the compression technique, the ciphertext sizes remain constant across all datasets. This is mainly because the client’s number of ciphertexts for the initial query matched the number of CW-encoded data bits. For BCC and the final inference response, only a single ciphertext was needed, as all intermediate data fit within 16,382 slots of a single ciphertext. By contrast, SilentWood’s ciphertext compression could reduce the number of required ciphertexts by a factor of repetitive data encoding, where the repetition was calculated by dividing the total number of slots in a ciphertext by: the total number of feature types multiplied by the CW-encoded bit-length. On average, using ciphertext compression reduced the ciphertext size from 85.75MB to 15.12MB in the case of 32-bit feature data bit-length. Table 9 shows the computation overheads for the server’s ciphertext decompression (Algorithm 5 in §C); the average times are 142 ms and 226 ms for 16-bit and 32-bit data bit lengths, respectively.

Blind Code Conversion: Table 9 also shows the computation overheads BCC (2 and 3). A majority of the overhead came from the

Benchmark	SoK-GGG				Baseline+B+K				Baseline+B+K+C			
	0ms	50ms	100ms	200ms	0ms	50ms	100ms	200ms	0ms	50ms	100ms	200ms
Spam	3.35s	5.95s	8.47s	13.44s	5.92s	6.89s	7.92s	10.11s	4.57s	5.26s	6.06s	7.70s
Steel	3.22s	5.56s	7.47s	11.91s	1.23s	2.40s	3.43s	5.57s	1.19s	1.98s	2.70s	4.31s
Breast	2.28s	2.69s	5.62s	9.16s	0.94s	2.08s	3.05s	5.30s	0.79s	1.81s	2.40s	3.94s
Heart	13.69s	23.26s	33.09s	52.88s	3.52s	4.57s	5.71s	7.92s	3.39s	4.11s	4.72s	6.34s
Defect	3.48s	6.39s	9.25s	15.06s	8.97s	9.99s	10.95s	13.27s	7.72s	8.38s	8.93s	10.48s
Bank	3.50s	6.45s	9.42s	15.96s	11.95s	13.06s	14.08s	16.25s	10.23s	10.95s	11.51s	13.00s
Pendigits	3.42s	5.47s	7.77s	12.49s	1.69s	2.87s	3.91s	6.08s	1.81s	2.56s	3.23s	4.74s
Ailerons	3.49s	6.56s	9.30s	16.15s	12.18s	13.15s	14.24s	16.36s	9.37s	10.08s	10.66s	12.17s
Credit	3.09s	5.20s	6.91s	11.84s	0.92s	2.06s	3.08s	5.30s	1.02s	1.76s	2.43s	3.93s
Satellite	3.04s	5.30s	7.54s	12.32s	1.05s	2.22s	3.29s	5.43s	1.11s	1.91s	2.61s	4.19s
Elevators	3.46s	6.24s	9.30s	15.21s	11.57s	12.72s	13.57s	15.64s	9.76s	10.48s	10.96s	12.38s
Telescope	3.16s	4.88s	6.53s	9.94s	0.58s	1.73s	2.81s	5.06s	0.83s	1.57s	2.25s	3.73s
MFeat	24.20s	41.57s	58.61s	95.23s	11.33s	12.47s	13.29s	15.76s	8.70s	9.53s	10.17s	12.22s
AVG.	5.64s	9.88s	13.79s	22.43s	5.53s	6.63s	7.64s	9.85s	4.65s	5.41s	6.05s	7.63s
SilentWood's Speedup	1.21x	1.83x	2.28x	2.94x	1.19x	1.20x	1.26x	1.29x	-	-	-	-

Table 10: The end-to-end inference time between the server and client over various RTTs (with a 32-bit feature size)

rotation operations to permute real SumPaths. The average times are 2282ms and 2362ms for 16-bit and 32-bit data bit lengths.

5.4 Inference Time over Various RTTs

Table 10 shows XGBoost’s end-to-end inference time for various RTTs. In the case of 50ms RTT, the time difference between Baseline + B + K (6.63s) and Baseline + B + K + C (5.41s) implies the 1.20x speedup achieved by ciphertext compression. SilentWood is faster than SoK-GGG by 1.83x, 2.28x, and 2.94x for RTT 50ms, 100ms, and 200ms respectively. SilentWood is faster than SoK-GGG by 1.21x on average even for RTT = 0ms, illustrating SilentWood’s computational efficiency.

6 Related Work

PDTE by Fully Homomorphic Encryption (FHE): XCMPPDTE [38] and SortingHat [19] rotate polynomial coefficients in a polynomial ring to homomorphically compare encrypted values, but the algorithm is not scalable over data bit-length; their supported bit-length is only up to 11~13 bits. RCC-PDTE [3] proposes a more efficient comparison operator based on CW encoding. However, its SumPath computation is incompatible with the score aggregation of decision forests and also incurs much overhead, both in terms of computation and communication, when handling a large number of trees.

PDTE by Two-party Computation (2PC): 2PC is a special case of multi-party computation (MPC) where a server and client compute the result of a common formula without revealing each other’s inputs to it. Brickell et al. [12] propose an efficient constant-round protocol based on oblivious transfer (OT), garbled circuit (GC), and additive homomorphic encryption. Kiss et al. [35] combined them with other protocols to create an efficient PDTE protocol. However, 2PC usually incurs a communication cost that grows exponentially with the tree depth because all tree paths need to be evaluated. Some of the later works addressed the issue of communication overhead by using oblivious RAM [47] or pseudo-random functions [5].

PDTE Extendable to Random Forest: HBDT [44] trains a decision tree homomorphically on a single outsourced server, using one-hot encoding for features to compare against thresholds. But one-hot encoding scales poorly: 32-bit inputs need 655 RLWE ciphertexts (19.7

GB for $N = 2^{14}$, $d = 2$), whereas SilentWood needs ~5 MB. BPDTE-CW [20] speeds RCC-PDTE’s batch comparison by using only CW digits equal to 1 per node; yet, communication grows by 17.7% over RCC-PDTE when the width increases from 11 to 16 bits. And since >85% of PDTE cost is computing/packing SumPath, faster comparisons help only to a limited extent. Both HBDT [44] and BPDTE-CW [20] use MultiplyPath (path conjugation) for forests, causing heavy cipher–cipher multiplications (Baseline, §5.1), whereas SilentWood uses SumPath with BCC to avoid them. Alouf et al. [4] build a leveled-HE [10]+threshold-encryption forest but support only a few trees (e.g., 3) with 8-bit data. Ma et al. [39] give an MPC-based PDTE (additive sharing, OT, GC) with $O(\text{depth})$ communications and leakage of tree counts/depths. Wu et al. [49] use additive HE and OT, but costs scale poorly with depth. Unlike these, SilentWood’s costs grow slowly with depth (mainly due to extra cipher–cipher additions) and do not leak tree count or depth.

Techniques Comparable to BCC: LWE-family scheme’s programmable bootstrapping (PBS) [18] enables the server to homomorphically convert encrypted plaintext values based on a mapping table. However, PBS suffers a large computation overhead because the LWE scheme does not support SIMD operations. Further, TFHE-PBS is feasible only for 2–5 bit values and applying to 8-bit circuits is too slow (e.g., hours per bootstrapping). In such a low-bit circuit design, even additions internally involve bit-wise slow multiplications. SilentWood avoids such a binary circuit design via BFV-based SIMD with BCC at the cost of 1 RTT, achieving 27.8× speedup over TFHE-based designs. Multiplying a random permutation matrix [48] to the intermediate ciphertext can give the same effect as random shuffling. However, homomorphic matrix-vector multiplications generically require $O(\sqrt{N})$ rotations and $O(N)$ multiplications [17], whereas SilentWood’s blind shuffling requires $O(\ell)$ rotations and no multiplication (where $\ell < N$ in general) and thus faster for gradient boosting inference.

Techniques Comparable to Ciphertext Compression: SortingHat’s [19] transciphering and Onion-ORAM’s [13] RLWE-to-RGSW conversion are designed for TFHE and fundamentally incompatible with BFV/BGV. SilentWood’s ciphertext compression supports SIMD-based addition and multiplication using BFV/BGV, unlike SortingHat/Onion-ORAM using TFHE, which is slow because it lacks

efficient batching. SortingHat's transciphering accounts for 35% of inference time and grows with tree depth; Onion-ORAM's ciphertext expansion adds 33–66% overhead (see Table 2 in their paper). SilentWood's decompression overhead is only 7.1% (Table 9), independent of depth, making it a more efficient compression method for BFV/BGV.

Techniques Comparable to Node Clustering: Several ML techniques prune decision trees to reduce inference overhead for resource-constrained embedded devices. ForestPrune [37] trims deeper layers across trees via global optimization, yielding compact ensembles with minimal accuracy loss. LOP [22] prunes entire trees and re-optimizes surviving leaf values to meet an accuracy budget. FIPE [1] removes redundant trees while guaranteeing functionally identical predictions. In contrast to these shape-modifying methods, SilentWood's node clustering preserves the trained tree's topology (depth, node count, tree count); it then groups similar thresholds per feature and forces them to use the same value, thereby shrinking the number of *distinct comparisons*. This approach is beneficial when a service provider must preserve model logic, interpretability, or certification workflows. SilentWood's node clustering could also complement existing pruning methods by both pruning branches and unifying similar-threshold values.

Other PDTE Protocols: MP2ML [8] uses mixed-mode protocols, which require costly conversions. Recent studies [23] show that avoiding such conversions improves performance. Since we found FHE best-suited for comparisons, we designed SilentWood as a pure-FHE protocol with only two rounds. NodeGuard [21] and Squirrel [32] focus on training, whereas SilentWood's emphasis is on low-latency and low-round inference.

7 Conclusion

SilentWood's private inference over gradient-boosting decision forests significantly enhances performance compared to existing methods. SilentWood's novel techniques include computation clustering to eliminate duplicate homomorphic computations, blind code conversion to preserve arithmetic compatibility for efficient tree score aggregation, and ciphertext compression to reduce the encrypted data size. SilentWood achieves an average private XGBoost inference time of $2.9x \sim 28.1x$ faster than state-of-the-art FHE or MPC-based protocols (i.e., Zama's concrete ML, RCC-PDTE, and SoK-GGG).

Ethical Considerations

Our work studies privacy-preserving inference for gradient boosting decision forests using only open-source UCI datasets [41], without involving personally identifying information. There is no real attack, no real harm occurred during this study. As with any cryptographic techniques, misuse is possible: we discourage unethically concealing discriminatory or harmful models.

Open Science

We will release the artifact to reproduce the experimental results illustrated in §5.

References

- [1] Free lunch in the forest: Functionally-identical pruning of boosted tree ensembles. 39:16488–16495, Apr. 2025.
- [2] Adi Akavia, Craig Gentry, Shai Halevi, and Margarita Vald. Achievable CCA2 relaxation for homomorphic encryption. *J. Cryptol.*, 38(1):5, 2025.
- [3] Rasoul Akhavan Mahdavi, Haoyan Ni, Dimitry Linkov, and Florian Kerschbaum. Level up: Private non-interactive decision tree evaluation using leveled homomorphic encryption. In *Proceedings of the 2023 ACM SIGSAC Conference on Computer and Communications Security, CCS '23*, page 2945–2958, New York, NY, USA, 2023. Association for Computing Machinery.
- [4] Asma Aloufi, Peizhao Hu, Harry W.H. Wong, and Sherman S.M. Chow. Blindfolded evaluation of random forests with multi-key homomorphic encryption. *IEEE Transactions on Dependable and Secure Computing*, 18(4):1821–1835, 2021.
- [5] Jianli Bai, Xiangfu Song, Shujie Cui, Ee-Chien Chang, and Giovanni Russello. Scalable private decision tree evaluation with sublinear communication. In *Proceedings of the ACM Asia Conference on Computer and Communications*, pages 843–857, 2022.
- [6] Jianli Bai, Xiangfu Song, Xiaowu Zhang, Qifan Wang, Shujie Cui, Ee-Chien Chang, and Giovanni Russello. Mostree: Malicious secure private decision tree evaluation with sublinear communication. In *Proceedings of the Annual Computer Security Applications Conference*, pages 799–813, 2023.
- [7] Christopher M. Bishop. *Pattern Recognition and Machine Learning (Information Science and Statistics)*. Springer-Verlag, Berlin, Heidelberg, 2006.
- [8] Fabian Boemer, Rosario Cammarota, Daniel Demmler, Thomas Schneider, and Hossein Yalame. Mp2ml: a mixed-protocol machine learning framework for private inference. In *Proceedings of the 15th International Conference on Availability, Reliability and Security, ARES '20*, New York, NY, USA, 2020. Association for Computing Machinery.
- [9] Raphael Bost, Raluca Ada Popa, Stephen Tu, and Shafi Goldwasser. Machine learning classification over encrypted data. In *Proceedings of the 22nd Network and Distributed System Security Symposium*, 2015.
- [10] Zvika Brakerski, Craig Gentry, and Vinod Vaikuntanathan. (leveled) fully homomorphic encryption without bootstrapping. In *Proceedings of the 3rd Innovations in Theoretical Computer Science Conference, ITCS '12*, page 309–325, New York, NY, USA, 2012. Association for Computing Machinery.
- [11] Leo Breiman. Random forests. *Machine Learning*, page 5, 2001.
- [12] Justin Brickell, Donald E. Porter, Vitaly Shmatikov, and Emmett Witchel. Privacy-preserving remote diagnostics. In *Proceedings of the 2007 ACM Conference on Computer and Communications Security*, pages 498–507, 2007.
- [13] Hao Chen, Ilaria Chillotti, and Ling Ren. Onion ring oram: Efficient constant bandwidth oblivious ram from (leveled) tffe. In *Proceedings of the 2019 ACM SIGSAC Conference on Computer and Communications Security, CCS '19*, page 345–360, New York, NY, USA, 2019. Association for Computing Machinery.
- [14] Hao Chen, Kim Laine, and Rachel Player. Simple encrypted arithmetic library - seal v2.1. In Michael Brenner, Kurt Rohloff, Joseph Bonneau, Andrew Miller, Peter Y.A. Ryan, Vanessa Teague, Andrea Bracciali, Massimiliano Sala, Federico Pintore, and Markus Jakobsson, editors, *Financial Cryptography and Data Security*, pages 3–18, Cham, 2017. Springer International Publishing.
- [15] Tianqi Chen and Carlos Guestrin. XGBoost: A scalable tree boosting system. In *Proceedings of the 22nd ACM SIGKDD International Conference on Knowledge Discovery and Data Mining, KDD '16*, page 785–794, New York, NY, USA, 2016. Association for Computing Machinery.
- [16] Nan Cheng, Naman Gupta, Aikaterini Mitrokotsa, Hiraku Morita, and Kazunari Tozawa. Constant-round private decision tree evaluation for secret shared data. *Proceedings on Privacy Enhancing Technologies*, 2024(1):397–412, 2024.
- [17] Jung Hee Cheon, Kyoohyung Han, Andrey Kim, Miran Kim, and Yongsoo Song. Bootstrapping for approximate homomorphic encryption. In Jesper Buus Nielsen and Vincent Rijmen, editors, *Advances in Cryptology – EUROCRYPT 2018*, pages 360–384, Cham, 2018. Springer International Publishing.
- [18] Ilaria Chillotti, Marc Joye, and Pascal Paillier. Programmable bootstrapping enables efficient homomorphic inference of deep neural networks. In Shlomi Dolev, Oded Margalit, Benny Pinkas, and Alexander Schwarzmann, editors, *Cyber Security Cryptography and Machine Learning*, pages 1–19, Cham, 2021. Springer International Publishing.
- [19] Kelong Cong, Debajyoti Das, Jeongeun Park, and Hilder V. L. Pereira. Sorting-hat: Efficient private decision tree evaluation via homomorphic encryption and transciphering. In *Proceedings of the 2022 ACM Conference on Computer and Communications Security*, pages 563–577, 2022.
- [20] Kelong Cong, Jiayi Kang, Georgio Nicolas, and Jeongeun Park. Faster private decision tree evaluation for batched input from homomorphic encryption. In Clemente Galdi and Duong Hieu Phan, editors, *Security and Cryptography for Networks*, pages 3–23, Cham, 2024. Springer Nature Switzerland.
- [21] Tianxiang Dai, Yufan Jiang, Yong Li, and Fei Mei. NodeGuard: A Highly Efficient Two-Party Computation Framework for Training Large-Scale Gradient Boosting Decision Tree. In *2024 IEEE Security and Privacy Workshops (SPW)*, pages 95–103, Los Alamitos, CA, USA, May 2024. IEEE Computer Society.

- [22] Laurens Devos, Timo Martens, Deniz Can Oruc, Wannes Meert, Hendrik Blockeel, and Jesse Davis. Compressing tree ensembles through level-wise optimization and pruning. In *Forty-second International Conference on Machine Learning*, 2025.
- [23] Abdulrahman Diaa, Lucas Fenaux, Thomas Humphries, Marian Dietz, Faezeh Ebrahimiaghazani, Bailey Kacsmar, Xinda Li, Nils Lukas, Rasoul Akhavan Mahdavi, Simon Oya, Ehsan Amjadian, and Florian Kerschbaum. Fast and private inference of deep neural networks by co-designing activation functions. In *33rd USENIX Security Symposium (USENIX Security 24)*, pages 2191–2208, Philadelphia, PA, August 2024. USENIX Association.
- [24] Léo Ducas and Damien Stehlé. Sanitization of FHE ciphertexts. In *EUROCRYPT (1)*, volume 9665 of *Lecture Notes in Computer Science*, pages 294–310. Springer, 2016.
- [25] Junfeng Fan and Frederik Vercauteren. Somewhat practical fully homomorphic encryption. *IACR Cryptology ePrint Archive*, page 144, 2012.
- [26] Junfeng Fan and Frederik Vercauteren. Somewhat practical fully homomorphic encryption. *Cryptology ePrint Archive*, 2012.
- [27] Yoav Freund and Robert E. Schapire. A decision-theoretic generalization of on-line learning and an application to boosting. In *Proceedings of the Second European Conference on Computational Learning Theory*, EuroCOLT '95, page 23–37, Berlin, Heidelberg, 1995. Springer-Verlag.
- [28] Jerome H. Friedman. Greedy function approximation: A gradient boosting machine. *The Annals of Statistics*, 29(5):1189–1232, 2001.
- [29] Jiaxuan Fu, Ke Cheng, Yuheng Xia, Anxiao Song, Qianxing Li, and Yulong Shen. Private decision tree evaluation with malicious security via function secret sharing. In *Proceedings of the 29th European Symposium on Research in Computer Security*, pages 310–330, 2024.
- [30] Craig Gentry. *A fully homomorphic encryption scheme*. PhD thesis, Stanford, CA, USA, 2009. AAI3382729.
- [31] Craig Gentry. Fully homomorphic encryption using ideal lattices. In *Proceedings of the 41st ACM Symposium on Theory of Computing*, pages 169–178, 2009.
- [32] Wen jie Lu, Zhicong Huang, Qizhi Zhang, Yuchen Wang, and Cheng Hong. Squirrel: A scalable secure Two-Party computation framework for training gradient boosting decision tree. In *32nd USENIX Security Symposium (USENIX Security 23)*, pages 6435–6451, Anaheim, CA, August 2023. USENIX Association.
- [33] Marc Joye and Fariborz Salehi. Private yet efficient decision tree evaluation. In *Proceedings of the 32nd IFIP Conference on Data and Applications Security and Privacy*, pages 243–259, 2018.
- [34] Kelong Cong and Jiayi Kang and Georgio Nicolas and Jeongeun Park. Faster private decision tree evaluation for batched input from homomorphic encryption. In *Proceedings of the 14th International Conference on Security and Cryptography for Networks*, pages 3–23, 2024.
- [35] Ágnes Kiss, Masoud Naderpour, Jian Liu, N. Asokan, and Thomas Schneider. Sok: Modular and efficient private decision tree evaluation. *Proceedings on Privacy Enhancing Technologies*, 2019(2):187–208, 2019.
- [36] Yehuda Lindell. How to simulate it - A tutorial on the simulation proof technique. In *Tutorials on the Foundations of Cryptography*, pages 277–346. Springer International Publishing, 2017.
- [37] Brian Liu and Rahul Mazumder. Forestprune: Compact depth-pruned tree ensembles. In Francisco Ruiz, Jennifer Dy, and Jan-Willem van de Meent, editors, *Proceedings of The 26th International Conference on Artificial Intelligence and Statistics*, volume 206 of *Proceedings of Machine Learning Research*, pages 9417–9428. PMLR, 25–27 Apr 2023.
- [38] Wen-jie Lu, Jun-jie Zhou, and Jun Sakuma. Non-interactive and output expressive private comparison from homomorphic encryption. In *Proceedings of the 2018 on Asia Conference on Computer and Communications Security, ASIACCS '18*, page 67–74, New York, NY, USA, 2018. Association for Computing Machinery.
- [39] Jack P. K. Ma, Raymond K. H. Tai, Yongjun Zhao, and Sherman S. M. Chow. Let's stride blindfolded in a forest: Sublinear multi-client decision trees evaluation. In *Proceedings of the 28th Network and Distributed System Security Symposium*, 2021.
- [40] Rasoul Akhavan Mahdavi and Florian Kerschbaum. Constant-weight PIR: Single-round keyword PIR via constant-weight equality operators. In *31st USENIX Security Symposium (USENIX Security 22)*, pages 1723–1740, Boston, MA, August 2022. USENIX Association.
- [41] Markelle Kelly, Rachel Longjohn, Kolby Nottingham. The UCI Machine Learning Repository, 2024. <https://archive.ics.uci.edu>.
- [42] Michael Kerrisk. Linux/UNIX system programming training, 2024. <https://man7.org/linux/man-pages/man8/tc-netem.8.html>.
- [43] Goldreich Oded. *Foundations of Cryptography: Volume 2, Basic Applications*. Cambridge University Press, USA, 1st edition, 2009.
- [44] Hojune Shin, Jina Choi, Dain Lee, Kyoungok Kim, and Younho Lee. Fully homomorphic training and inference on binary decision tree and random forest. In *Computer Security – ESORICS 2024: 29th European Symposium on Research in Computer Security, Bydgoszcz, Poland, September 16–20, 2024, Proceedings, Part III*, page 217–237, Berlin, Heidelberg, 2024. Springer-Verlag.
- [45] Raymond K. H. Tai, Jack P. K. Ma, Yongjun Zhao, and Sherman S. M. Chow. Privacy-preserving decision trees evaluation via linear functions. In *Proceedings of the 22nd European Symposium on Research in Computer Security*, pages 494–512, 2017.
- [46] Anselme Tueno, Yordan Boev, and Florian Kerschbaum. Non-interactive private decision tree evaluation. In *Proceedings of the 34th IFIP Conference on Data and Applications Security and Privacy*, pages 174–194, 2020.
- [47] Anselme Tueno, Florian Kerschbaum, and Stefan Katzenbeisser. Private evaluation of decision trees using sublinear cost. *Proceedings on Privacy Enhancing Technologies*, 2019(1):266–286, 2019.
- [48] Wikipedia. Permutation matrix, 2024. https://en.wikipedia.org/wiki/Permutation_matrix.
- [49] David J. Wu, Tony Feng, Michael Naehrig, and Kristin E. Lauter. Privately evaluating decision trees and random forests. *Proceedings on Privacy Enhancing Technologies*, 2016(4):335–355, 2016.
- [50] Hao Yang, Shiyu Shen, Wangchen Dai, Lu Zhou, Zhe Liu, and Yunlei Zhao. Phantom: A cuda-accelerated word-wise homomorphic encryption library. *IEEE Transactions on Dependable and Secure Computing*, pages 1–12, 2024.
- [51] Andrew Chi-Chih Yao. Protocols for secure computations (extended abstract). In *Proceedings of the 23rd Symposium on Foundations of Computer Science*, pages 160–164, 1982.
- [52] Andrew Chi-Chih Yao. How to generate and exchange secrets (extended abstract). In *Proceedings of the 27th Annual Symposium on Foundations of Computer Science*, pages 162–167, 1986.
- [53] Zama. Concrete ML, 2024. <https://docs.zama.ai/concrete-ml>.

A Comparison Operator based on CW-encoding

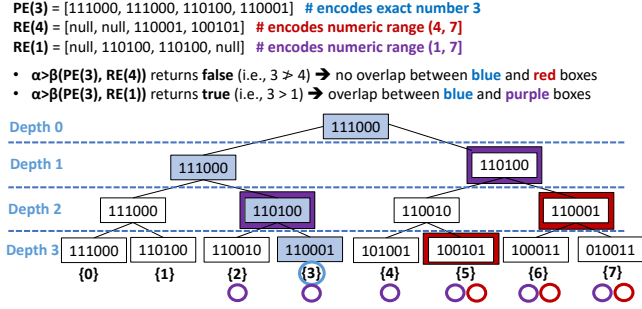


Figure 8: RCC-PDTE [3]’s examples of value comparison ($3 > 4$? $3 > 1$?), where each tree node’s label is CW-encoded.

```

We run this function at each tree node, where  $\alpha$  = feature,  $\beta$  = threshold
bool  $\alpha > \beta(PE(\alpha), RE(\beta))$ : # Given  $PE(\alpha)$  and  $RE(\beta)$ , determine if  $\alpha > \beta$ 
    int accumulator = 0;
    for (int i = 0; i < PE( $\alpha$ ).length; i++)
        accumulator += is_equal(PE( $\alpha$ )[i], RE( $\beta$ )[i])
    return accumulator; # returns 1 if  $\alpha > \beta$ ; 0 otherwise
bool is_equal(x, y) # returns 1 if  $x == y$ ; 0 otherwise
    int h = 0;
    for (int i = 0; i < L; i++) # L: bit length of the encoded values
        h += x[i] * y[i]
    m = 1;
    for (int i = 0; i < H; i++) # H: Hamming weight (number of 1s)
        m *= h - i
    int H_FACTORIAL = H*(H-1)*(H-2)*...3*2*1 # a pre-computed constant
    return (H_FACTORIAL)-1 * m # where m is either H_FACTORIAL or 0
    
```

Figure 9: An arithmetic circuit of comparing two input numbers (α, β) encoded by CW-encoding ($PE(\alpha), RE(\beta)$).

The state-of-the-art value comparison algorithm based on FHE is the one proposed by RCC-PDTE [3]. Figure 8 illustrates a high-level idea of how this works: two numbers to be compared are encoded as a vector of node labels that form a complete binary tree (CBT, which is different from a decision tree). CBT’s each leaf node corresponds to the target number to encode. The CBT has 8 leaves and can encode any numbers between 0 and 7. Based on this CBT, RCC-PDTE proposes two number encoding schemes: PE (point encoding) and RE (range cover encoding). PE encodes an exact number corresponding to a particular leaf node in a CBT as a vector of node labels. The elements of this vector tell the path from the root to a target leaf node. In Figure 8, we PE-encode 3 as PE vector $[111000, 111000, 110100, 110001]$ (visualized as blue nodes and a blue circle). The CBT’s each node label is encoded as constant-weight encoding [40] (CW-encoding), which is essentially a Hamming-weight encoding whose base-2 representation always contains the same frequency of 1s for any target value to encode. We will later explain why we use CW-encoding for labeling.

Unlike PE encoding, RE encodes a range of values as a vector such that each of its elements corresponds to a specific node in each tree depth (or can be NULL if no node is chosen at that depth), and the encoded range of values is the set of all descendant leaves of the nodes in the vector. In Figure 8, we RE-encode range (4, 7] as RE vector $RE(4) = [null, null, 110001, 100101]$ (visualized as red nodes),

whose each element’s descendant leaves collectively cover value range $\{5, 6, 7\}$ (red circle). As another example, we RE-encode range (1, 7] as $RE(1) = [null, 110100, 110100, null]$ (purple nodes), whose descendant leaves collectively cover value range $\{2, 3, 4, 5, 6, 7\}$ (purple circles). Notably, the upper bound of the range encoded by RE is always the right-most leaf value in CBT (e.g., 7 in case of Figure 8).

Based on this CBT setup, to evaluate the condition $\alpha > \beta$, we determine whether two vectors $PE(\alpha)$ and $RE(\beta)$ share any common node (i.e., same node label at the same depth of CBT). If yes, then $\alpha > \beta$ holds; otherwise $\alpha \leq \beta$. For example, $PE(3)$ and $RE(4)$ have no common node at any depth, which visually implies that the blue path of $PE(3)$ has no overlap with the red boundary of $RE(4)$ (i.e., $3 \leq 4$). On the other hand, $PE(3)$ and $RE(1)$ have a common node at depth 2 (110100), which visually implies that the blue path of $PE(3)$ has an overlap with the purple boundary of $RE(1)$ (i.e., $3 > 1$). This value comparison logic is implemented in the upper dashed box of Figure 9. Within this function, the for-loop statement can be executed with FHE as a series of $(+, \cdot)$ operations, and we further detail the `is_equal` function’s internal logic in the lower dashed box, which again comprises only $(+, \cdot)$ operations. Therefore, the entire value comparison operation can be performed by FHE with the target numbers being encrypted ciphertexts. In particular, `is_equal` assumes that the CBT’s each node label is encoded as CW-encoding. Note that all for-loops in these functions have a deterministic number of looping, because the conditional variables for looping (`.length`, `L`, and `H`) are statically known values. The benefit of using CW encoding in this comparison algorithm is that during the FHE computation, we can effectively fix the number of multiplicative depth (fixed to $\lceil \log H \rceil + 2$) required for the `is_equal` operation regardless of the bit-length of input data (x, y).

B Security Analysis: Blind Code Conversion

Our protocol achieves privacy against both semi-honest clients and malicious servers.³ In particular, the client only learns the final class scores and some hyperparameters of the server’s model, while the server learns essentially nothing about the client’s features. Below we formally prove security with respect to each type of corruption when the protocol is instantiated with a sanitized FHE scheme.

The idealized functionality \mathcal{F}_{BCC} of the protocol is defined as follows:

- The client chooses its input for the classification.
- The server chooses its decision forest model, including some hyperparameters such as the frequency distribution f and the number of SumPaths ℓ .
- The client obtains the final class scores computed from the decision forest and the hyperparameters f and ℓ .

Security Against Corrupted Client: We demonstrate how the client’s view may be simulated using only its own input, the hyperparameters and the final class scores. The client’s view consists of its own input, its random coins, and the transcript of the protocol [36]. Formally, we have

$$\text{view}_{\text{CInt}}(x, y, \lambda) = (x, r, c_1, c_2),$$

where x holds the client’s private features, y is the server’s private model, λ is the security parameter, r is the collection of the client’s random coins, c_1 is the ciphertext holding the padded and shuffled SumPath values, and c_2 is the ciphertext holding the final class scores.

We require a sanitization algorithm, which transforms a ciphertext in a manner that preserves the message, while removing all information about the evaluated circuit. In other words, when sanitizing two ciphertexts that decrypt to the same message, the outputs are statistically close (hence indistinguishable). We refer to Ducas and Stehlé [24] for a formal treatment of sanitization. Assuming that c_1 and c_2 are sanitized, we can build a simulator for the client’s view as follows:

- The simulator copies the value of x from its input.
- The simulator generates r uniformly at random.
- The plaintext m_1 underlying c_1 is independent of the other entries of the client’s view (because it is shuffled using the server’s random coins). Therefore, the simulator can generate m_1 according to the desired frequency distribution f and number of SumPaths ℓ . It then generates the encryption key from the client’s random coins, and it encrypts and sanitizes m_1 . Due to the sanitization property, the resulting ciphertext is indistinguishable from the actual c_1 .
- The simulator encrypts and sanitizes the final class scores. Due to the sanitization property, the resulting ciphertext is indistinguishable from the actual c_2 .

Security Against Corrupted Server: SilentWood can be modeled as a client-aided outsourcing protocol. Akavia et al. [2] show that such a protocol achieves privacy if at least one of the following conditions is satisfied:

- It is cleartext computable (all plaintexts/cleartexts are functions of the client’s input) and it is instantiated with a CPA-secure FHE scheme.

³Privacy against malicious clients can be achieved by attaching a proof of well-formedness to all keys and ciphertexts.

- It is instantiated with a funcCPA-secure FHE scheme.

The first condition is not satisfied in SilentWood, because the plaintexts depend on the server’s model and its random shuffle. However, Akavia et al. [2] show that sanitized CPA-secure schemes are funcCPA-secure. Therefore, security can be proven in one of these situations: (i) BFV is funcCPA-secure; or (ii) BFV is CPA-secure and all ciphertexts are sanitized before sending them to the server.

B.1 Comparing Score Aggregation Overhead

	BCC	MultiplyPath
CMult	0	$O(\ell)$
PMult	$O(\log N) \approx O(1)$	$O(\ell)$
Rotate	$O(\ell + \log N) \approx O(\ell)$	0
CAdd	$O(\log \ell + \log N) \approx O(\log \ell)$	$O(\log \ell)$
RTTs	1	0

Table 11: Comparing the runtime overhead of leaf score aggregation based on BCC vs. MultiplyPath.

	BCC	MultiplyPath
CMult	0	$O(d)$
PMult	$O(\log N) \approx O(1)$	$O(1)$
Rotate	$O(\log N) \approx O(1)$	0
CAdd	$O(\log \ell)$	$O(\log \ell)$

Table 12: Circuit depth (i.e., critical path) of each type of operation.

N is the number of plaintext slots in a ciphertext, ℓ is the total number of tree paths, and d is the tree depth (i.e., path length). In this time complexity analysis, we assume a complete binary tree. Therefore, there are a total of $2\ell - 1$ nodes. In practical FHE, $\log N$ is fixed to be between 13 and 15; thus, $O(\log N) \approx O(1)$.

Table 11 shows the time complexity of score aggregation based on BCC and MultiplyPath. As illustrated in Algorithm 2, score aggregation based on BCC requires ℓ rotations and $\log \ell$ additions to randomly permute and aggregate ℓ real SumPaths (line 6), and 1 addition to merge them with randomly permuted dummy SumPaths (line 13). The overhead of $\log N$ rotations and $\log N$ plaintext-ciphertext multiplications occur during score aggregation (line 6, 7, and 8 in Algorithm 3), but this overhead is fixed and small in practice because $\log N$ is fixed to be between 14 and 16. Additionally, BCC involves one round-trip communication between the server and the client. During score aggregation in Algorithm 3, BCC requires $O(\log N) \approx O(1)$ ciphertext-to-plaintext multiplications to aggregate the final score (line 8).

In contrast, score aggregation based on MultiplyPath requires $2\ell - 1$ ciphertext-to-ciphertext multiplications to compute all MultiplyPaths of the tree, comprising $2\ell - 1$ edges, $2\ell - 1$ ciphertext-to-plaintext multiplications to weight each path result with the corresponding leaf value, and ℓ ciphertext-to-ciphertext additions to sum them up. Since all these operations are performed locally by the server, no round-trip communication with the client is needed. However, the dominant cost arises from the $2\ell - 1$ ciphertext-to-ciphertext multiplications, as the CMult operation is the most computationally expensive and consumes the largest noise budget among all (i.e., it is generally 10 times slower than PMult or Rotate).

Table 12 shows the circuit depth (i.e., the critical path) of score aggregation based on BCC and MultiplyPath. In the case of BCC, the critical path of $\log \ell$ CAdd operations is negligibly small, so the actual critical path is $\log N$ Rotate operations that occur during the final score aggregation in the for-loop (line 6) in Algorithm 3. But again, this is small and fixed because $\log N$ is fixed to be between 13 and 15. Note that although BCC requires ℓ rotations when permuting ℓ real SumPaths in the for-loop (line 8) in Algorithm 2, each of its iterations is independent and thus can run in parallel, which is equivalent to consuming a single circuit depth for all iterations. With multi-core processors or GPUs, this for-loop can also run efficiently in parallel. On the other hand, the critical path of MultiplyPath is d CMult operations during path evaluation. This is a significant computational bottleneck because, as the tree depth grows linearly, the computational overhead grows polynomially.

C Homomorphic Ciphertext Decompression

Algorithm 5 Ciphertext Decompression

Input: $encDataArrList$, $dataInitIndices$, $gapList$, $repetition$
 $encDataArrList \leftarrow []$ ▷ decompressed encrypted array list
 $encCDataArrIdx \leftarrow 0$ ▷ current compressed ciphertext index
for $encCDataArr \in encCDataArrList$ **do** ▷ for each compressed ciphertext
 for $repeatRound \in [0, \dots, repetition - 1]$ **do**
 $maskPt \leftarrow [0, \dots, 0]$
 for $info \in dataInitIndices$ **do** ▷ create the masking plaintext
 $keepIndex \leftarrow info.startIndex + gapList[repeatRound]$
 $maskPt[keepIndex] \leftarrow 1$
 end for
 $encDataArr \leftarrow PMult(encCDataArr, maskPt)$
 $encRotArr \leftarrow encDataArr$
 for $repeatIndex \in [0, \dots, repetition - 1]$ **do** ▷ restore the encoding of 'repetition'
 repetitions
 if $repeatIndex \neq repeatRound$ **then**
 $encRotated \leftarrow Rotate(encRotArr, gapList[repeatIndex])$
 $encDataArr \leftarrow Add(encDataArr, encRotated)$
 end if
 end for ▷ At this point, $encDataArr$ has been decompressed
 $encDataArrList.append(encDataArr)$
 end for
end for
Output: $encDataArrList$ ▷ decompressed ciphertext list

D Additional Evaluations

	Comparison Time	Total Inference Time	Fraction of Comparison Time
Spam	5.26s	6.14s	85.6%
Steel	4.46s	5.39s	82.7%
Breast	4.49s	5.32s	84.4%
Heart	20.37s	24.00s	84.9%
Defect	5.55s	6.41s	86.6%
Bank	5.67s	6.58s	86.2%
PenDigits	4.83s	5.82s	83.0%
Ailerons	5.62s	6.56s	85.7%
Credit	4.42s	5.24s	84.3%
Satellite	4.68s	5.49s	85.2%
Elevators	5.56s	6.49s	85.7%
Telescope	4.03s	5.00s	80.1%
MFeat	37.51s	45.37s	82.7%
AVG.	8.65s	10.29s	84.1%

Table 13: SoK-GGG’s Comparison Times and Total Inference Times

As we showed in Table 10, SoK-GGG’s computation time (without the communication cost) for private inference is large: 5.64 seconds on average. This cost primarily includes the time for garbled circuit operations in the comparison phase: OT extension for input values, circuit garbling (server-side), and circuit evaluation (client-side). Table 13 additionally shows SoK-GGG’s inference time and the fraction of time spent on comparisons at tree nodes. If we apply node clustering to SoK-GGG, the reduction ratio of nodes linearly reduces the amount of computation spent on the OT extension. Let α be the ratio of comparisons before node clustering to comparisons after node clustering, and let β be the time spent on comparisons relative to the total time spent in SoK-GGG. Let t be the time spent in SoK-GGG’s garbled circuit for comparisons. Then, SoK-GGG’s computation time for comparison with node clustering is expected to run in $\frac{(\beta \cdot t)}{\alpha} + (1 - \beta) \cdot t$.

	Validation Set Size	Node Reduction Rate	Test Set Accuracy	Abortion Rate
Spam	5%	71%	91%	30%
	10%	69%	93%	40%
	20%	72%	95%	35%
	30%	74%	98%	40%
Steel	5%	91%	100%	0%
	10%	91%	100%	0%
	20%	91%	100%	0%
	30%	91%	100%	0%
Breast	5%	84%	93%	9%
	10%	84%	91%	9%
	20%	78%	100%	23%
	30%	72%	100%	23%
Heart	5%	98%	62%	14%
	10%	94%	62%	29%
	20%	96%	59%	14%
	30%	93%	67%	43%
Defect	5%	74%	61%	70%
	10%	79%	62%	60%
	20%	76%	70%	60%
	30%	81%	52%	50%
Bank	5%	54%	90%	74%
	10%	62%	91%	61%
	20%	68%	91%	55%
	30%	62%	93%	68%
PenDigits	5%	79%	98%	38%
	10%	77%	97%	50%
	20%	71%	97%	56%
	30%	69%	97%	69%
Ailerons	5%	88%	93%	52%
	10%	89%	94%	56%
	20%	89%	94%	52%
	30%	89%	95%	52%
Credit	5%	66%	62%	0%
	10%	66%	62%	0%
	20%	66%	62%	0%
	30%	62.5%	75%	9%
Satellite	5%	81%	100%	10%
	10%	79%	100%	13%
	20%	75%	100%	26%
	30%	75%	100%	26%
Elevators	5%	92%	94%	57%
	10%	90%	93%	57%
	20%	89%	94%	64%
	30%	90%	94%	79%
Telescope	5%	94%	100%	0%
	10%	94%	100%	0%
	20%	94%	100%	0%
	30%	94%	100%	0%
MFeat	5%	76%	91%	27%
	10%	71%	91%	30%
	20%	65%	92%	42%
	30%	66%	89%	45%
	5%	65%	91%	52%

Table 14: Node clustering with various validation set sizes (5%~35%)